HDG

BUILDING MATERIALS

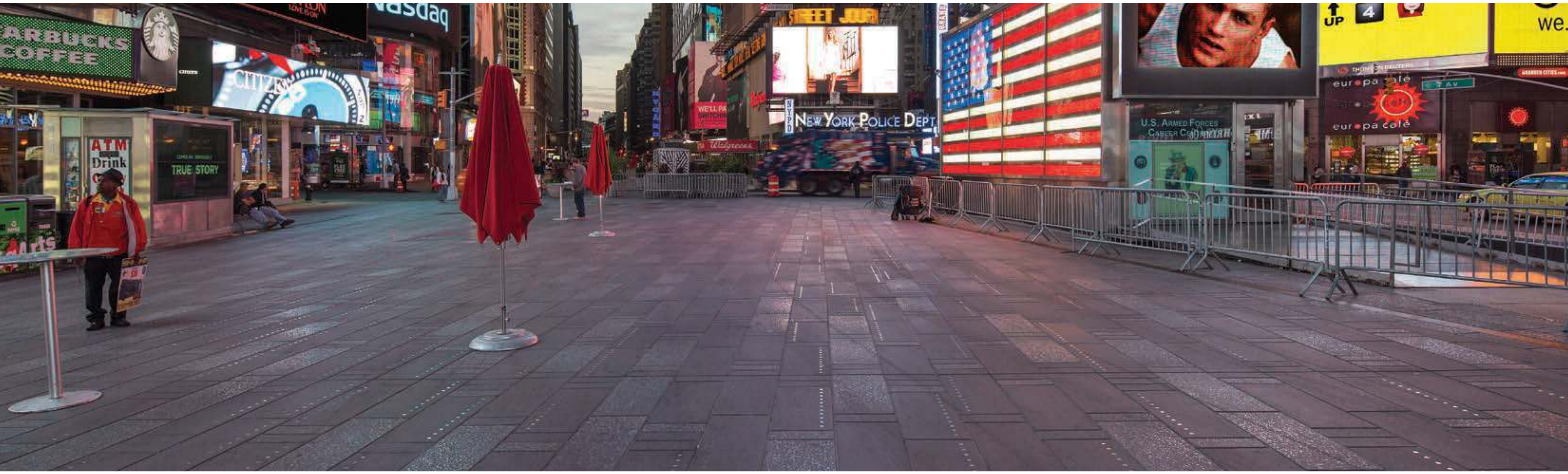

ARCHITECTURAL PAVERS
TECHNICAL MANUAL

HDG
BUILDING MATERIALS

THE PRODUCTS OFFERED IN THIS CATALOG
ARE MANUFACTURED IN WAUSAU, WI, BY
HDG'S PARTNER FACTORY

HDG Building Materials
Happy Valley, OR 97086
503.360.9551

HDGBUILDINGMATERIALS.COM

Concrete-based pavers with recycled glass or recycled porcelain may qualify for LEED credits that may contribute toward your project certification.

HDG Building Materials is an architect and builder's best resource for structural concrete pavers. We believe superior products make their mark on projects. But, we also are confident that people make a difference. When you add HDG to your extended team you gain our design and contracting backgrounds. We work closely with you and your clients on material selection and constructive solutions. It is part of our HDG Difference.

Our elegant and durable pavers combined with Buzon adjustable screw-jack pedestals create unforgettable and inviting spaces. Whether you seek bold, contemporary design or timeless beauty, our team will turn your vision into a lasting work of art.

CONTENTS

PAVER PRODUCT DATA

All HDG TECH Series pavers are subject to rigorous testing and manufactured to uphold the industry's tightest performance tolerances. Available in countless sizes and thicknesses – and with the ability to manufacture any size desired – HDG's high-quality concrete pavers bring big visions to life with beauty that's built to last.

SIZE AND WEIGHTS

Standard available sizes square pavers (nominal):
12", 16", 18", 24", 30", 36", and 42"

Standard available sizes rectangular pavers (nominal):
Widths: 3", 4", 6", 9", 12", 15", 16", 18", 24", 30", and 36"
Lengths: 12", 16", 18", 24", 30", 36", 42", and 48"
Thickness: 2" up to 4" -- Standard thickness 2", 2-3/4", 3", 4"
Weight: 24 to 48 lbs./sq. ft.

Dimensional tolerance: +/- 1/16" (Length, width, height, convex, concave). Custom sizes and thickness, available upon request.

TESTING

PROPERTY	STANDARD TESTING VALUE	ADVANCED TESTING VALUE	TEST METHOD
Compressive Strength	> 8,000 PSI avg. with no individual unit less than 7,000 PSI	> 9,500 PSI avg. with no individual unit less than 8,500 PSI	ASTM C 140
Water Absorption	< 6%	< 4%	ASTM C 140
Flexural Strength	> 800 PSI avg.	> 800 PSI avg.	ASTM C 293-14
Freeze/Thaw	< 0.1% loss of dry weight (50 cylces)	< 0.1% loss of dry weight (50 cycles)	ASTM C 1262
Center Load	1,850 lbs.	2,000 lbs.	WTCL 99

PAVER DIMENSIONS

PAVER SIZES	Joint	2"	2 1/4"	2 1/2"	2 3/4"	3"	4"
3x12"	4mm	**Standard**					**Standard**
4x8"	4mm					**Standard**	
4x12"	4mm	**Standard**					**Standard**
6x12"	4mm	**Standard**	Specialty	Specialty	**Standard**	**Standard**	**Standard**
6x16"	NA	Specialty	Specialty	Specialty	Specialty		
6x24"	4mm	**Standard**			**Standard**	**Standard**	**Standard**
8" Hex	1.5mm	**Standard**	Specialty	Specialty	Specialty		**Standard**
8x24"	4mm	**Standard**			**Standard**		
9x12"	6.5mm	Specialty	Specialty	Specialty	Specialty	**Standard**	
12x18"	4mm						
12x24"	4mm						**Standard**
15x9" Trap	4mm					**Standard**	
15x30"	3mm			Specialty	Specialty		

PAVER DIMENSIONS

PAVER SIZES	Joint	2"	2 1/4"	2 1/2"	2 3/4"	3"	4"
16x16"	NA	Specialty	Specialty	Specialty	Specialty		
18x18"	3mm	**Standard**	Specialty	Specialty	Specialty		
18x36"	3mm				**Standard**		
24x24"	4mm					**Standard**	
24x36"	3mm	**Standard**	Specialty	Specialty	Specialty		
30x30"	3mm		Specialty	Specialty	**Standard**		
40x40"	3mm					**Standard**	

3" x 12" x 2", PAVER

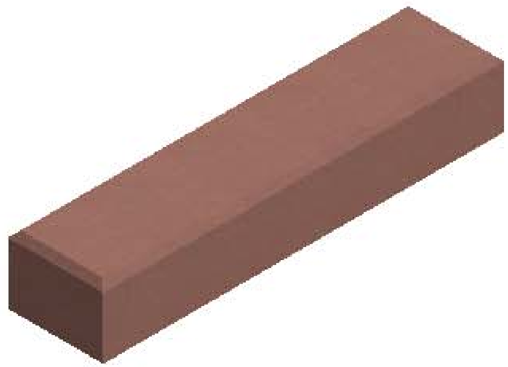

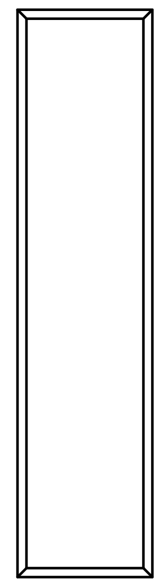

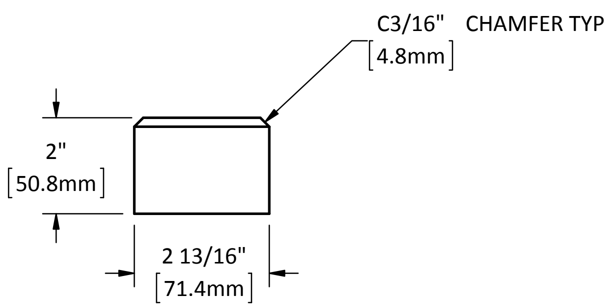

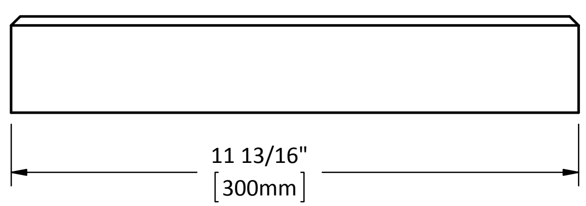

4" x 8" x 3", PAVER

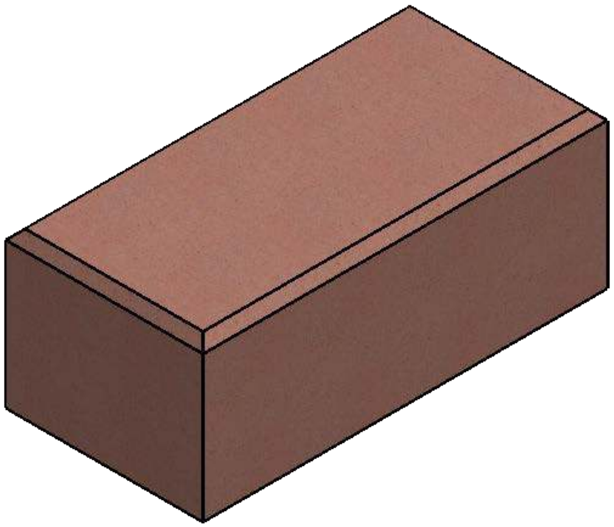

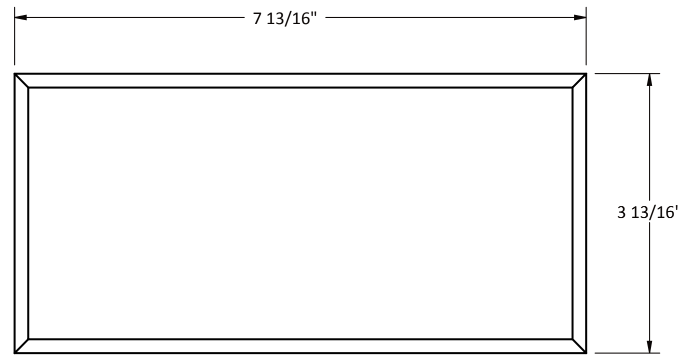

1 TOP VIEW

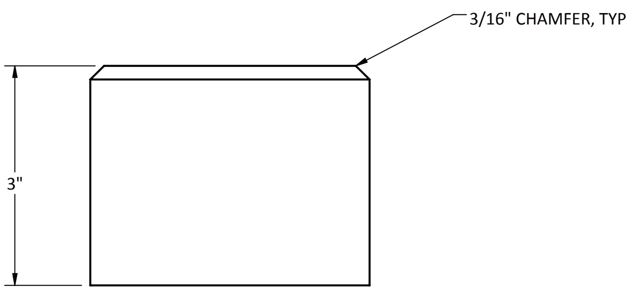

3 LEFT VIEW

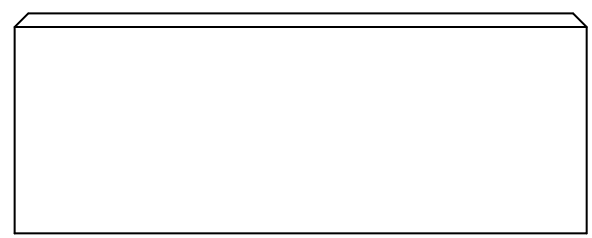

2 FRONT VIEW

4" x 12" x 2", PAVER

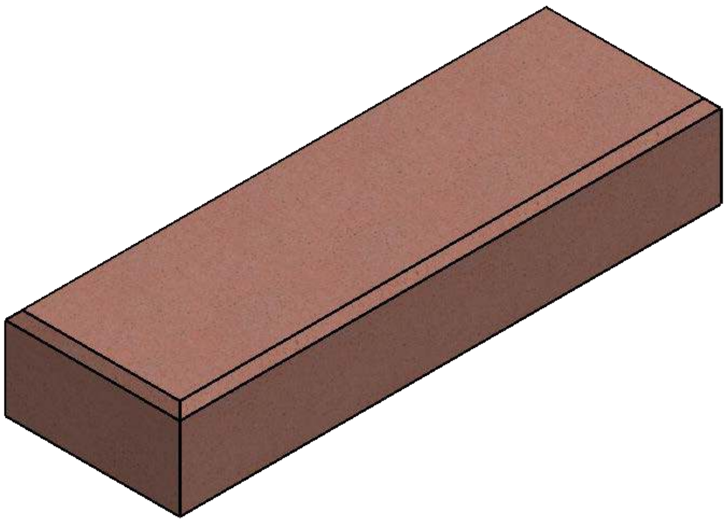

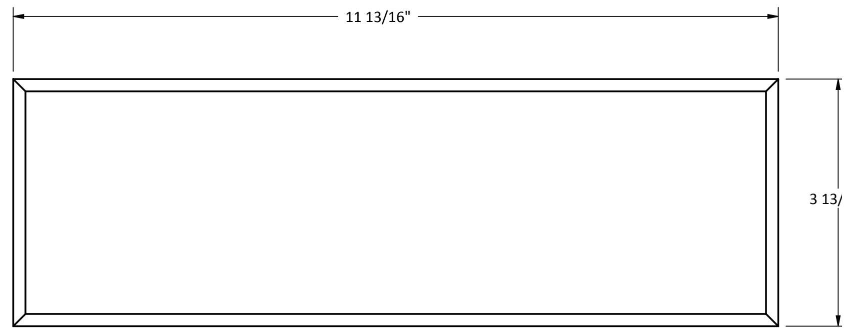

1 TOP VIEW

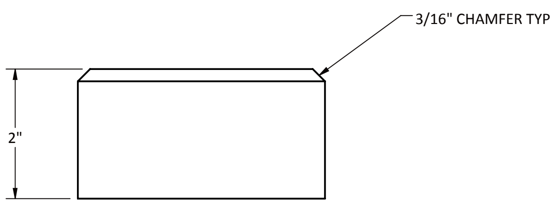

3 LEFT VIEW

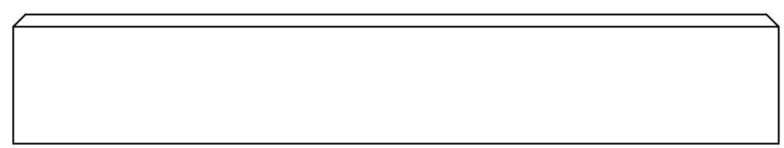

2 FRONT VIEW

6" x 12" x 2", PAVER

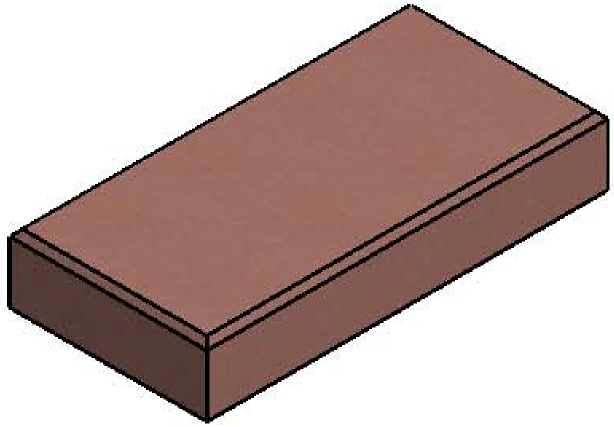

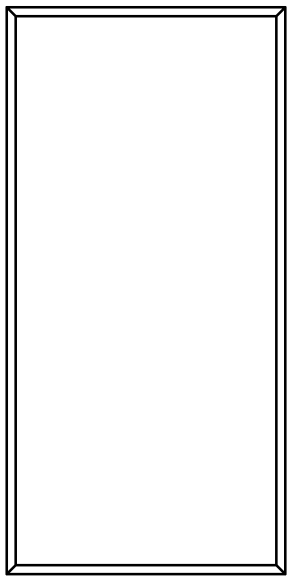

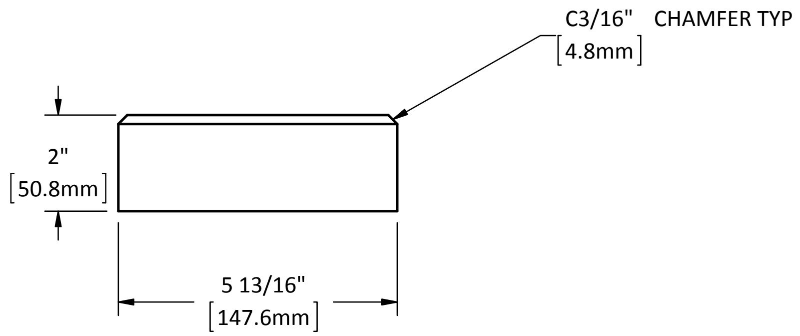

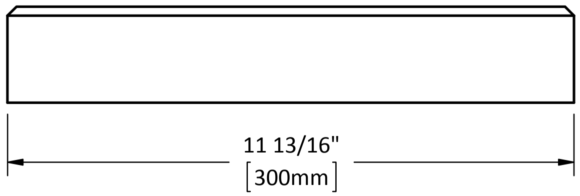

6" x 18" x 2 ¾", PAVER

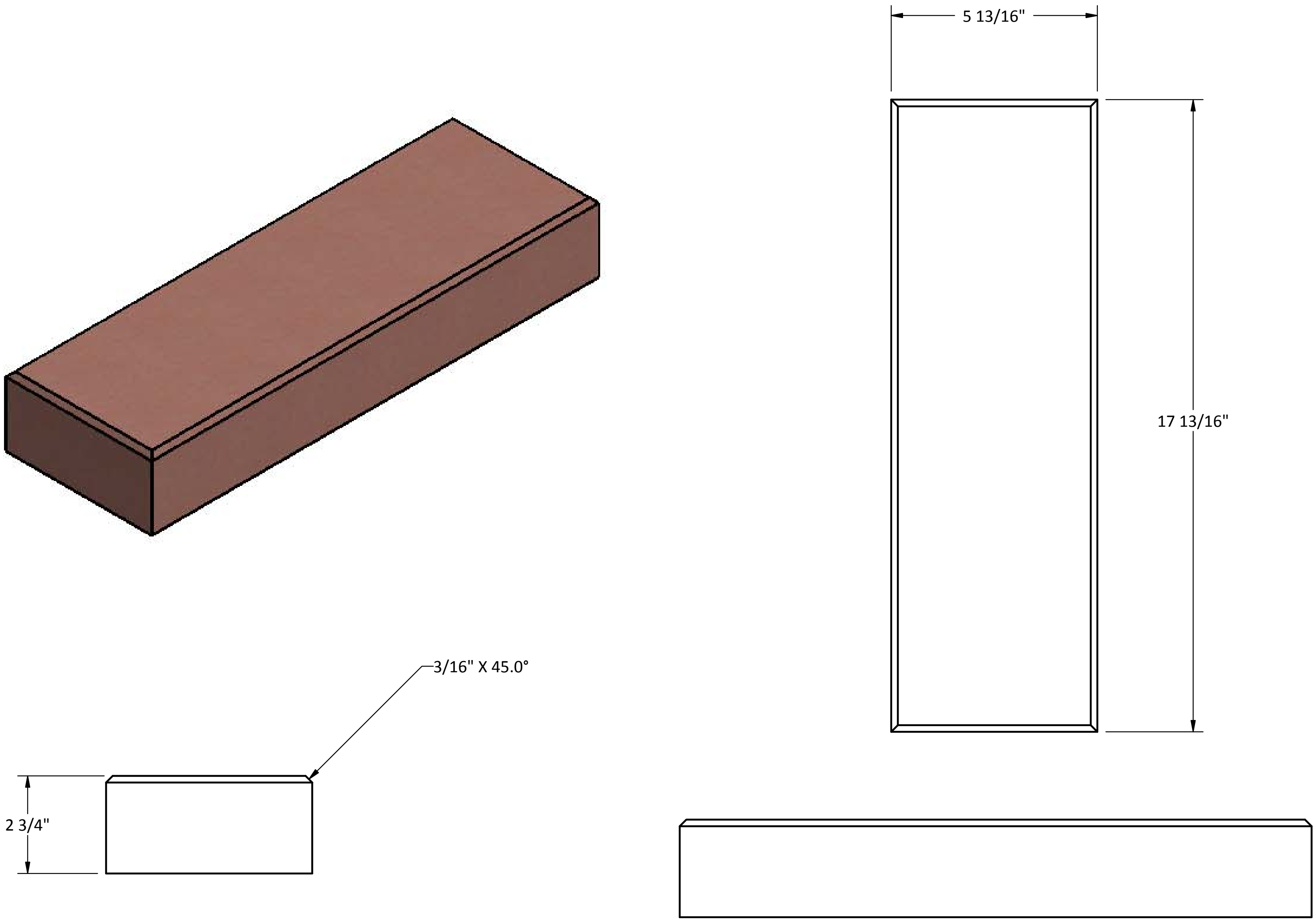

6" x 24" x 2", PAVER

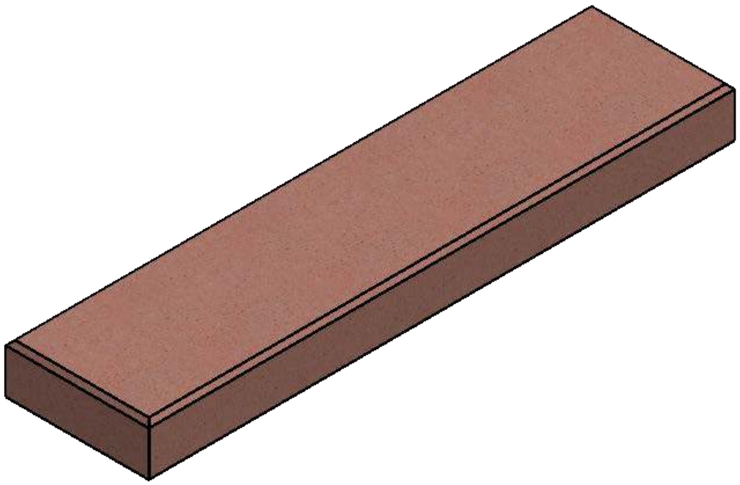

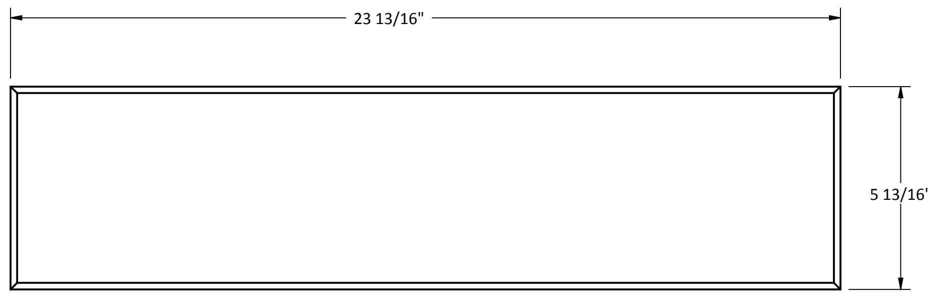

1 TOP VIEW

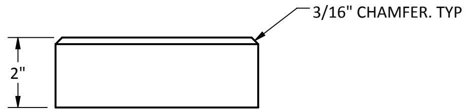

3 LEFT VIEW

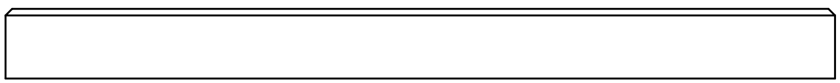

2 FRONT VIEW

6" x 36" x 2 ¾", PAVER

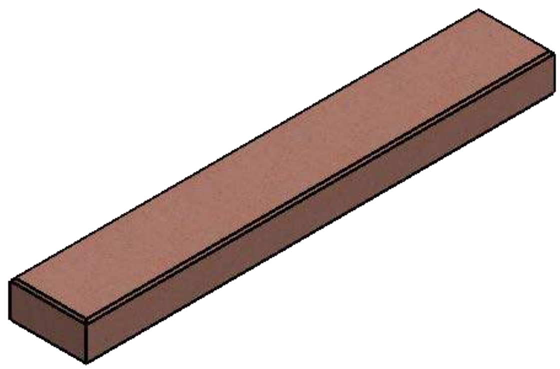

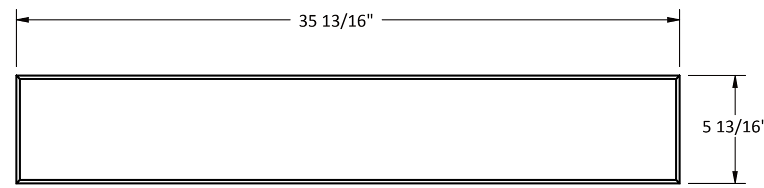

1 TOP VIEW

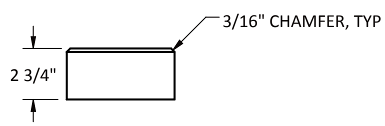

3 LEFT VIEW

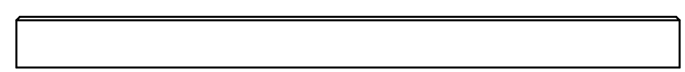

2 FRONT VIEW

8" HEX x 2", PAVER

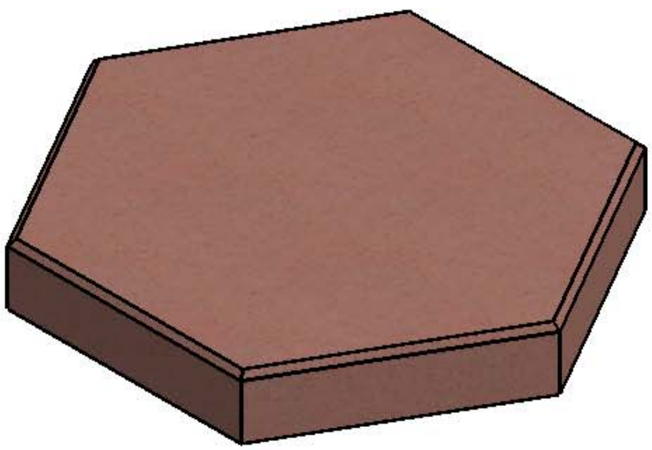

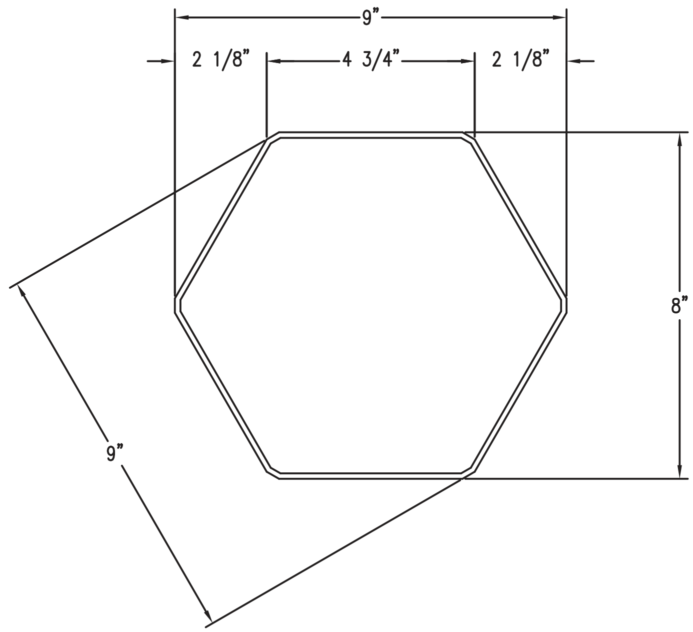

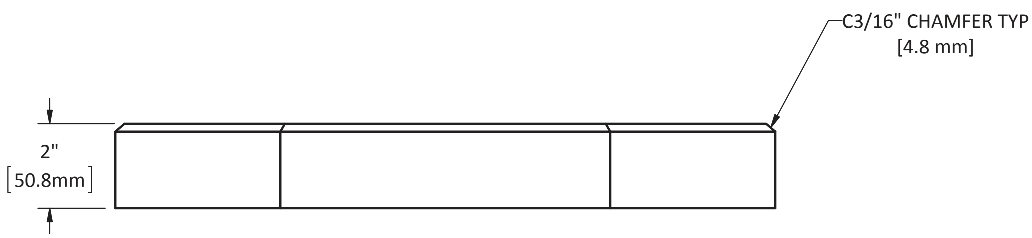

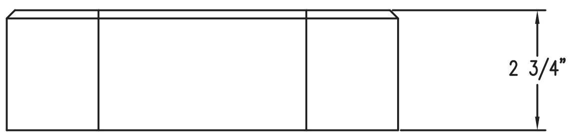

DETAIL FOR VEHICULAR USE

9" x 12" x 3", PAVER

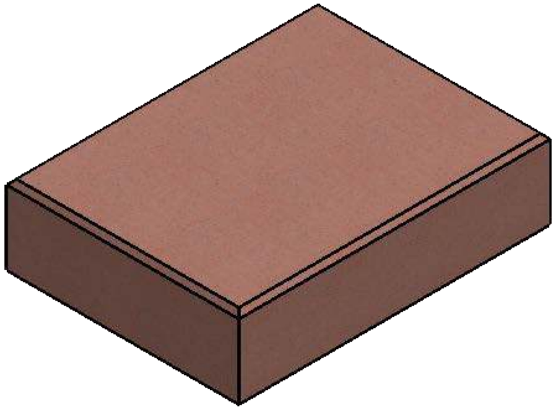

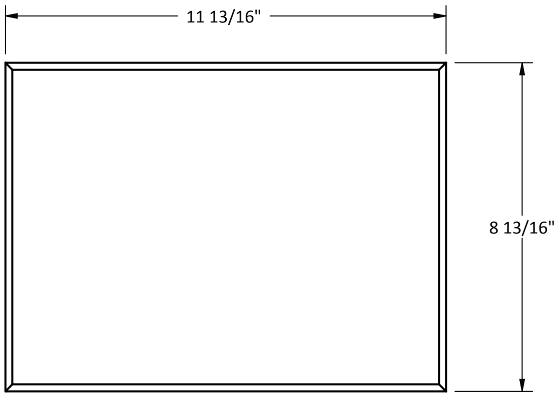

1 TOP VIEW

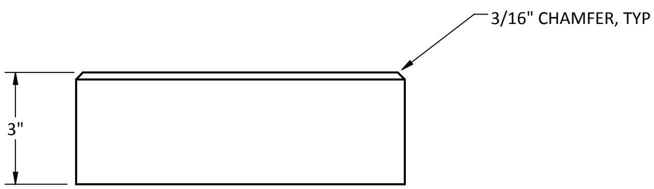

3 LEFT VIEW

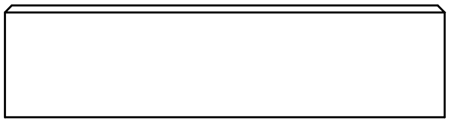

2 FRONT VIEW

12" x 12" x 2", PAVER

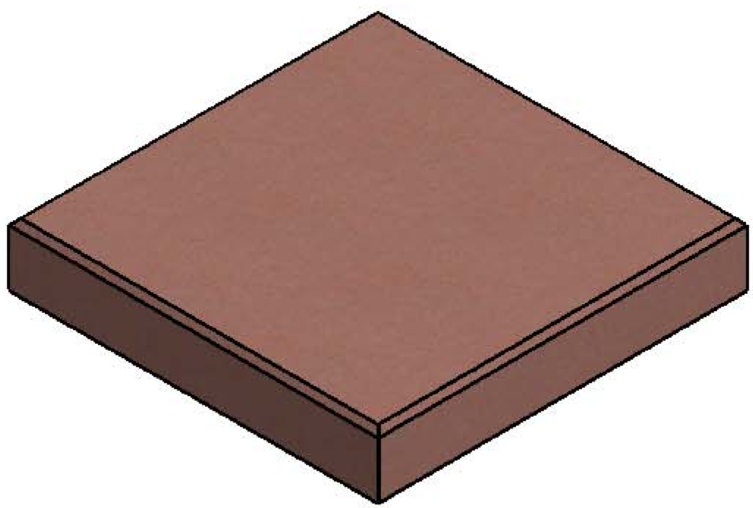

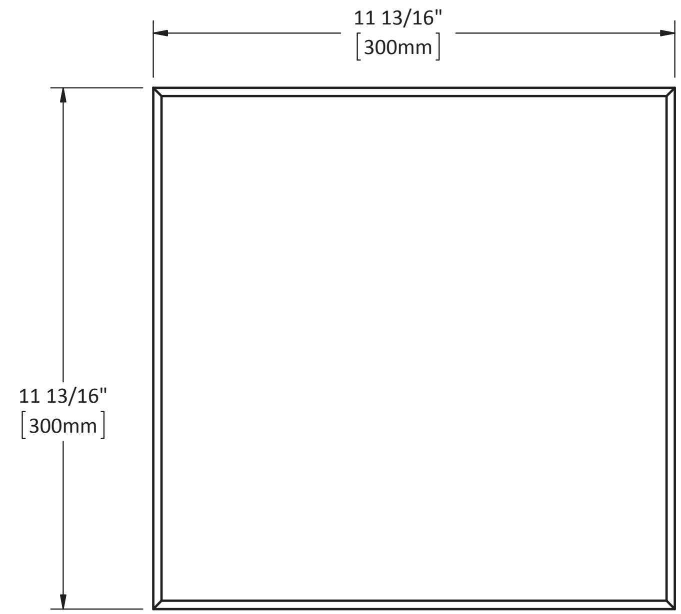

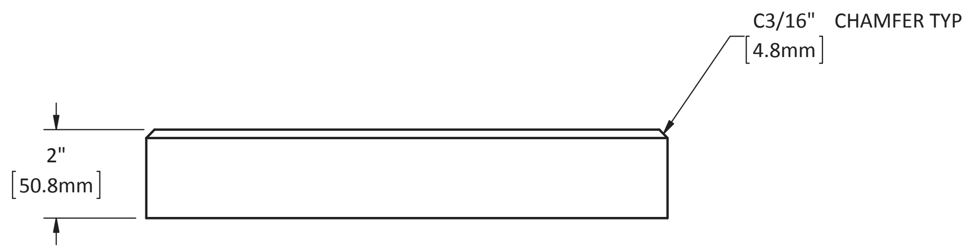

12" x 12" x 3", PAVER

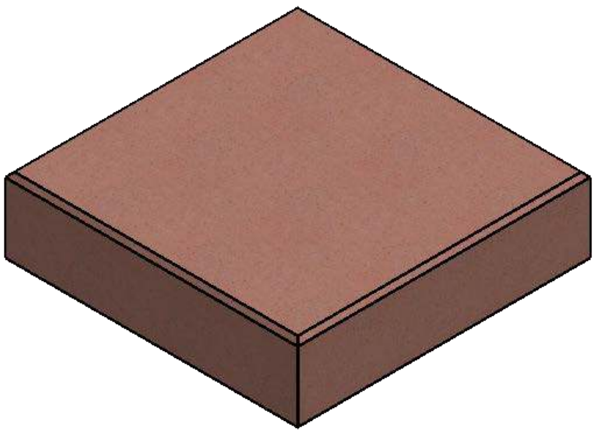

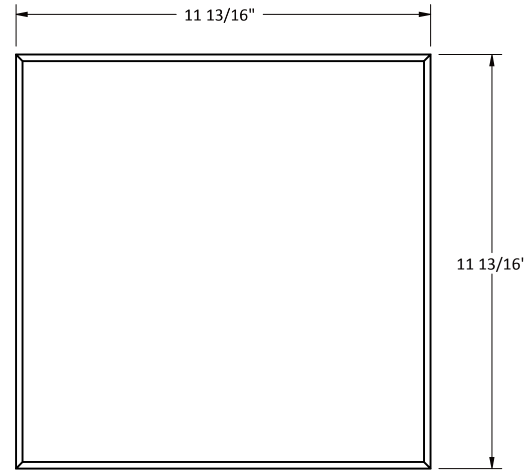

1 TOP VIEW

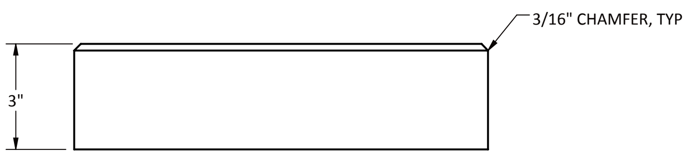

3 LEFT VIEW

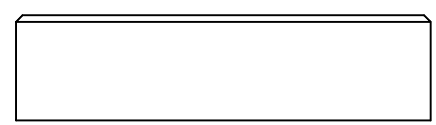

2 FRONT VIEW

12" x 24" x 2", PAVER

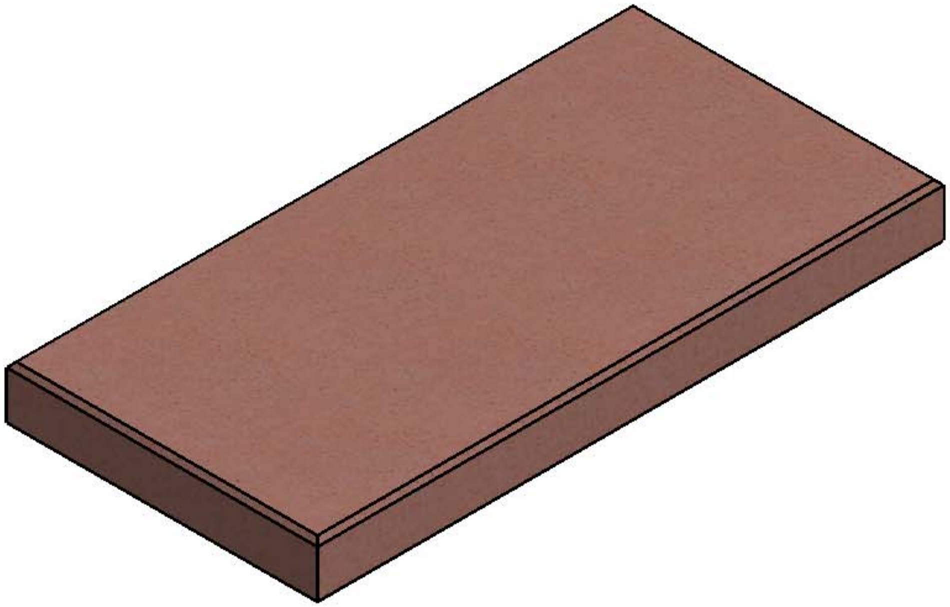

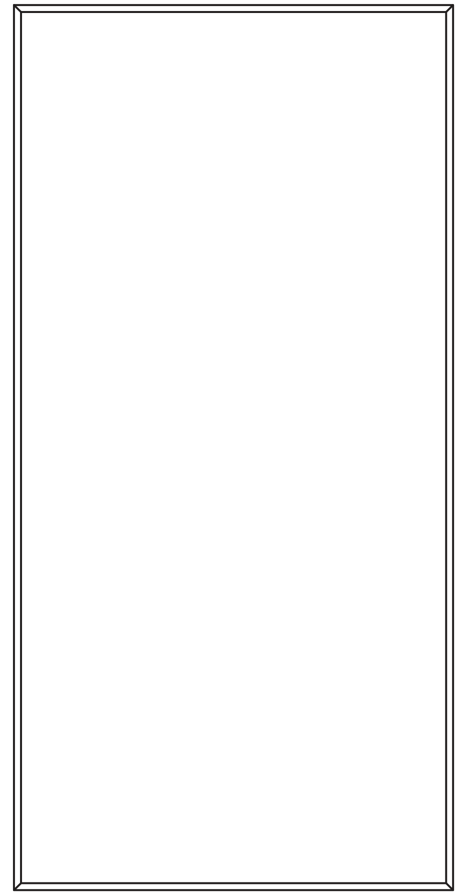

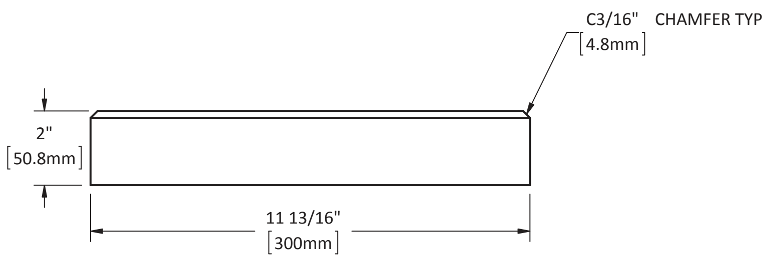

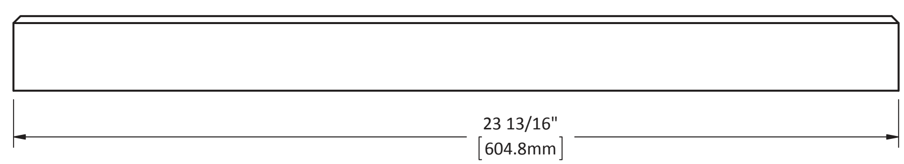

12" x 48" x 2 ¾", PAVER

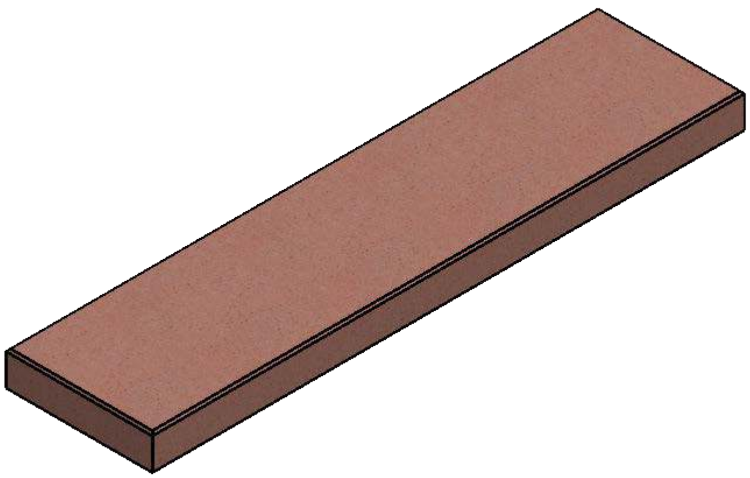

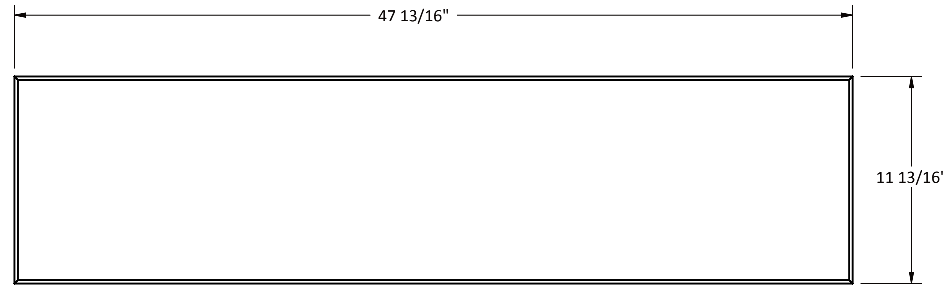

1 TOP VIEW

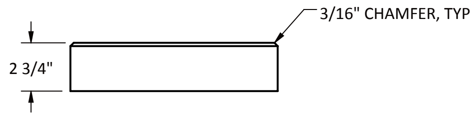

3 LEFT VIEW

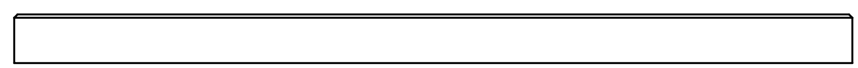

2 FRONT VIEW

15" x 30" x 2", PAVER

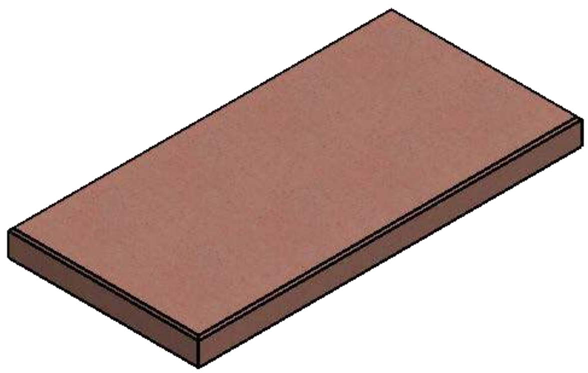

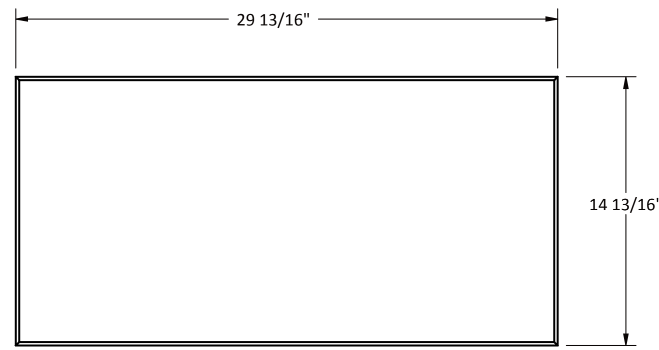

1 TOP VIEW

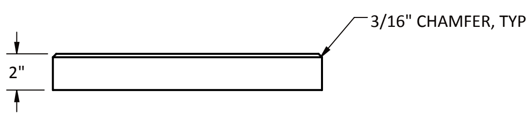

3 LEFT VIEW

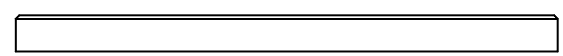

2 FRONT VIEW

18" x 18" x 2", PAVER

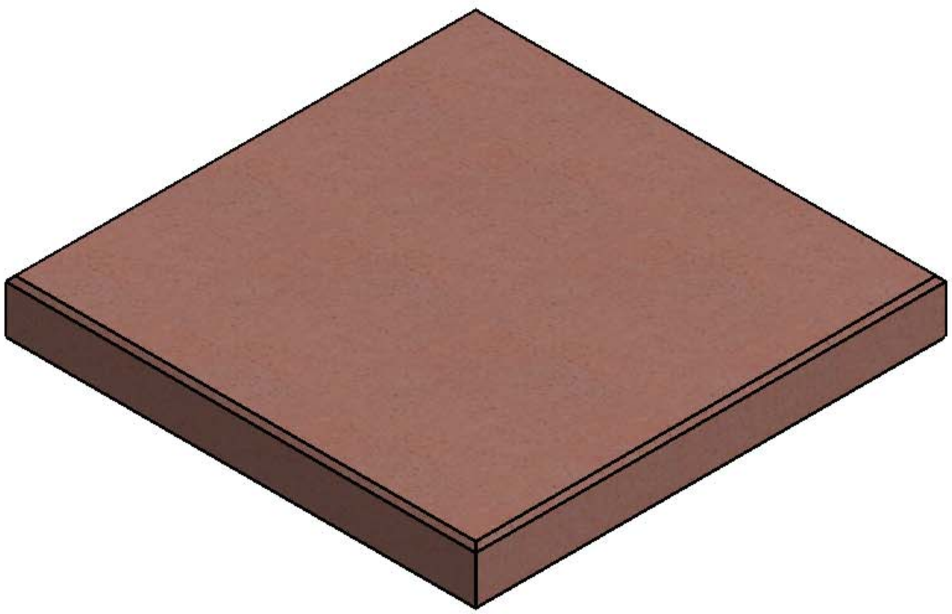

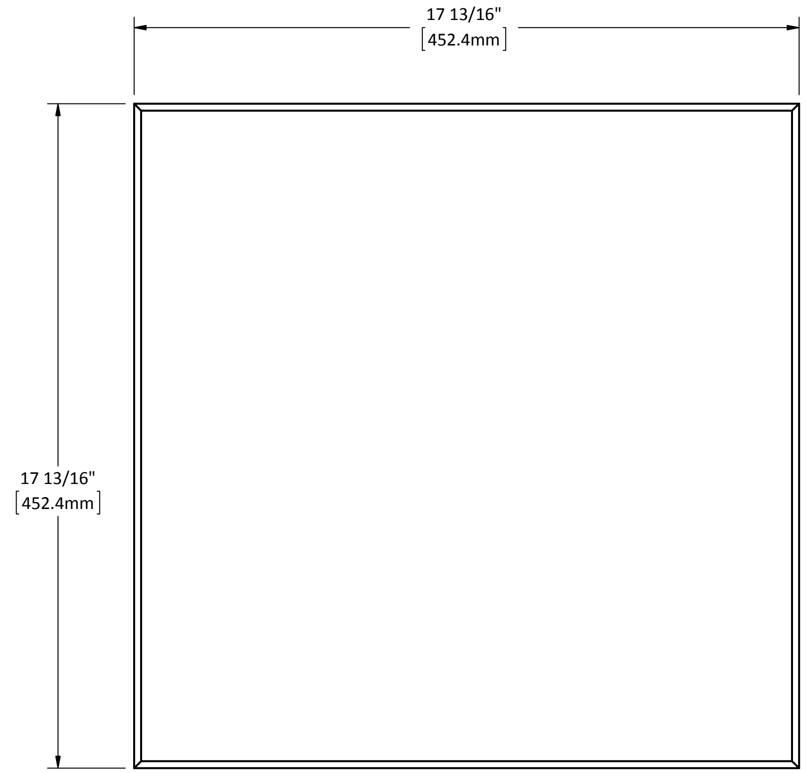

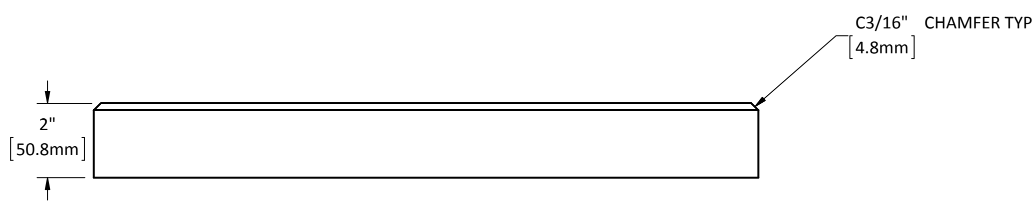

18" x 36" x 2 ¾", PAVER

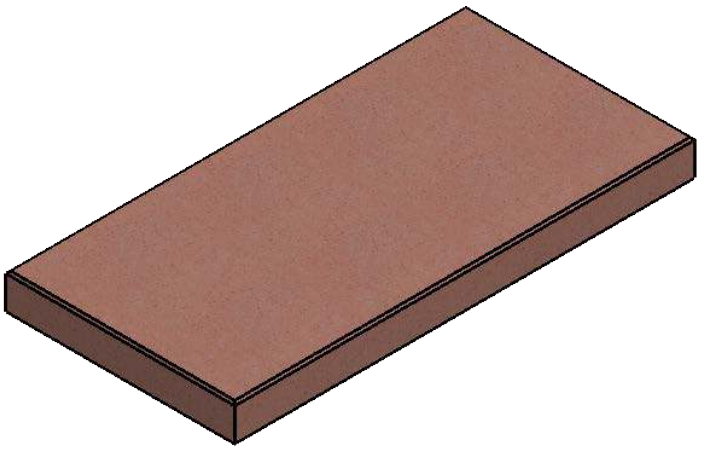

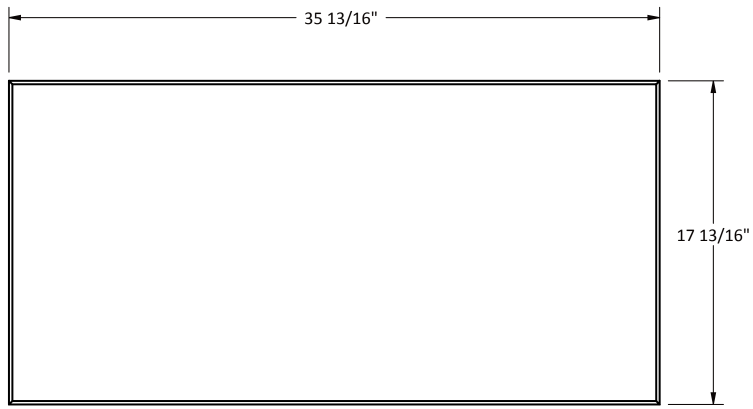

1 TOP VIEW

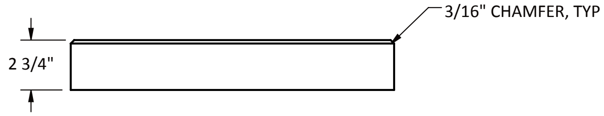

3 LEFT VIEW

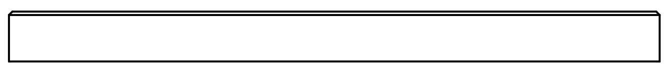

2 FRONT VIEW

24" x 24" x 2", PAVER

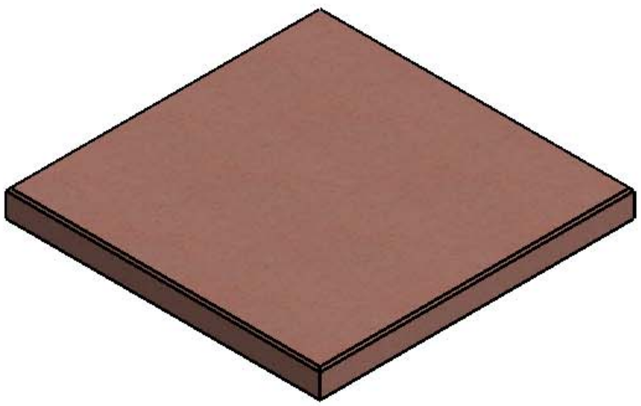

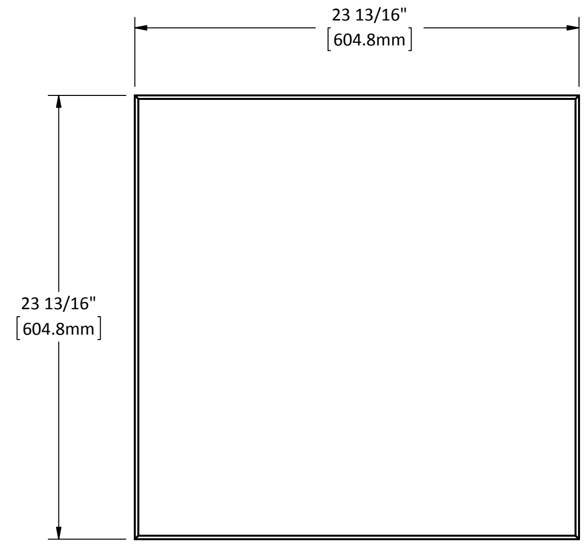

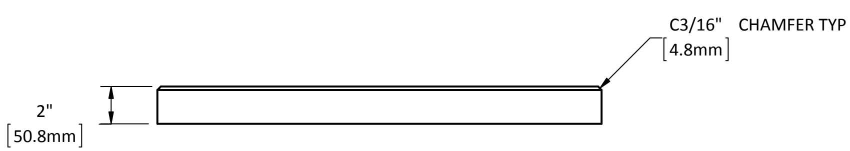

24" x 36" x 2", PAVER

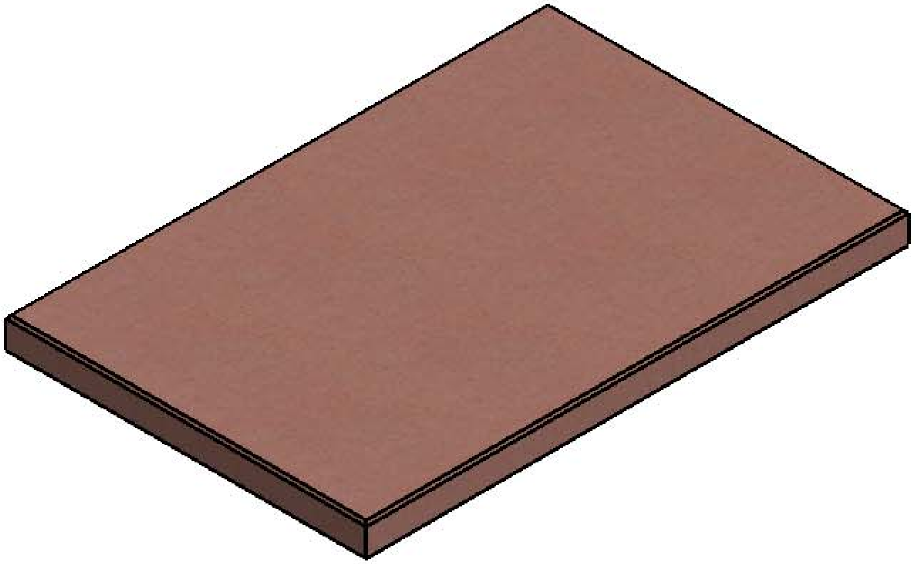

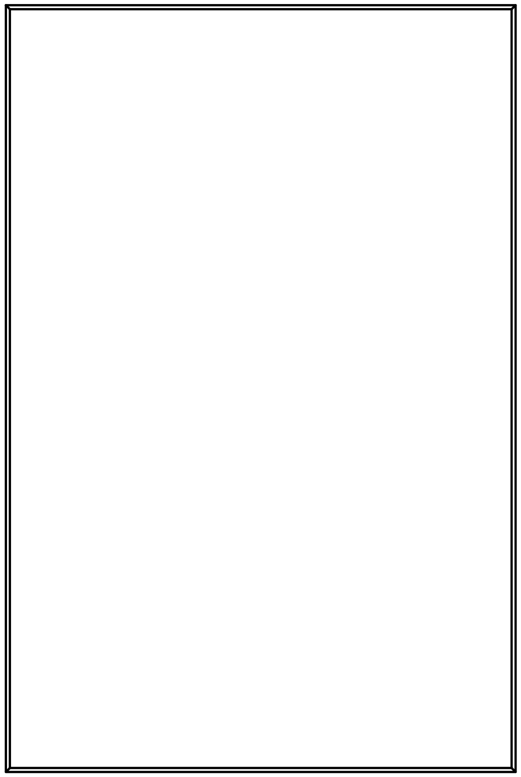

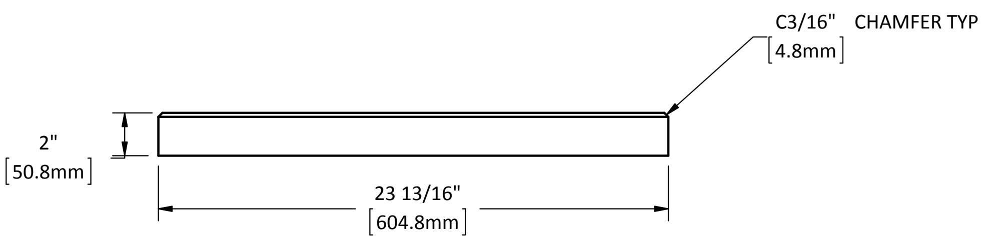

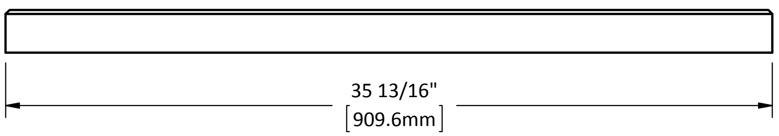

42" x 42" x 4", PAVER

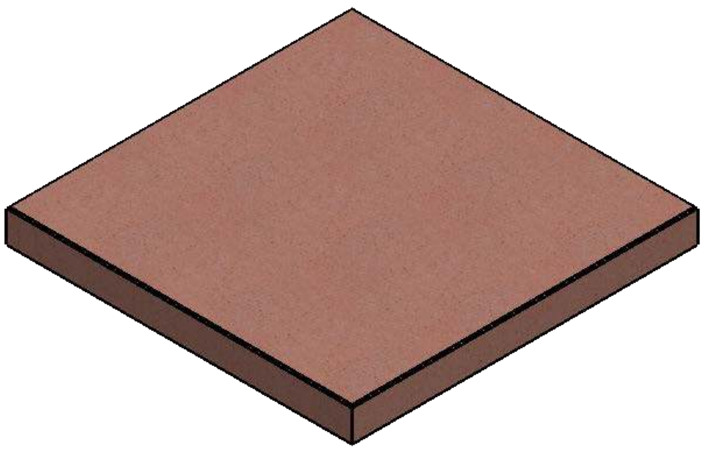

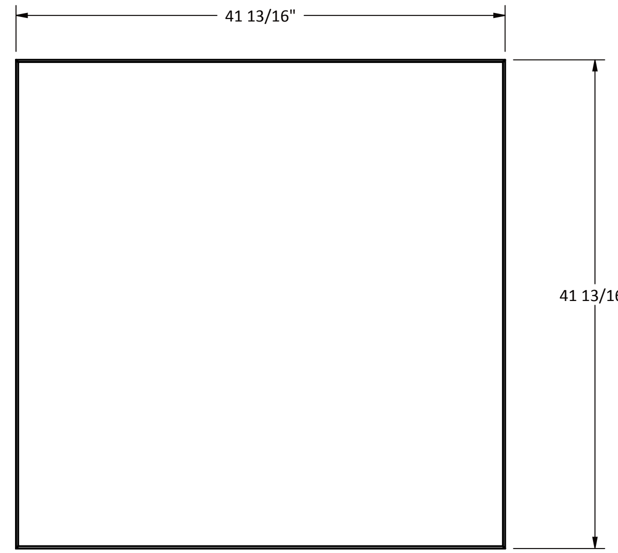

1 TOP VIEW

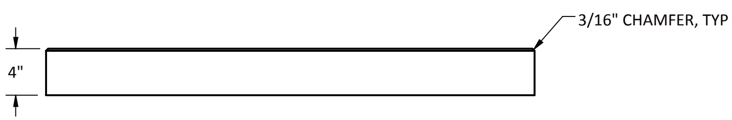

3 LEFT VIEW

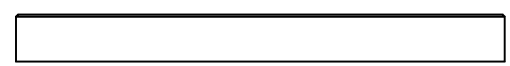

2 FRONT VIEW

WALL OF WIND TEST RESULTS

Rooftop and balcony spaces can be alluring, functional additions to any building, but powerful wind uplift poses a constant safety threat, capable of dislodging building parts and sending them flying dangerously through the air.

Working with the world's leading wind experts, all of HDG's TECH Series paving products are tested against hurricane-condition wind speeds and proven to perform.

Engineering Structures 44 (2012) 260-270

Contents lists available at SciVerse ScienceDirect

ENGINEERING STRUCTURES

journal homepage: www.elsevier.com/locate/engstruct

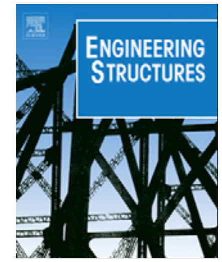

FULL-SCALE AERODYNAMIC TESTING OF A LOOSE CONCRETE ROOF PAVER SYSTEM

Aly Mousaad Aly [a,b,c], Girma T. Bitsuamlak [a,b,c,*], Arindam Gan Chowdhury [b,c]

[a] *Department of Civil and Environmental Engineering, University of Western Ontario, London, ON, Canada*

[b] *Laboratory for Wind Engineering Research (LWER), International Hurricane Research Center (IHRC), Florida International University (FIU), Miami, FL 33174, USA*

[c] *Department of Civil and Environmental Engineering (CEE), Florida International University (FIU), Miami, FL 33174, USA*

ARTICLE INFO

Article history:
Received 9 September 2010
Revised 8 May 2012
Accepted 9 May 2012
Available online 13 July 2012

Key words:
Full-scale aerodynamic testing
Flat roof
Loose concrete roof paver
Wall of Wind
Wind pressure

ABSTRACT

The paper presents an experimental study to assess wind induced pressure on full-scale loose concrete roof pavers by using Wall of Wind, a large-scale hurricane testing facility at Florida International University. Experimental tests were conducted on full-scale concrete pavers mounted on a test building to evaluate wind-induced external and underneath pressures acting on the pavers. The study shows that roof pavers could be subjected to significant uplifting wind forces due to negative pressures. In corner and edge areas of the roof, pressure differences produced net uplift on the pavers, at design wind speed, that was greater than the individual weight of the pavers. The study provides new insights by testing the actual roofing material at high wind speeds in a controlled environment and also showed that locking the pavers together can mitigate the issues at corners and edges by increasing the weight of the pavers that acts together to counterbalance the net uplift pressure.

1. Introduction

Hurricane winds cause economic losses, which can exceed $30 billion dollars each year in the United States, and the loss of many lives. Hurricane winds compete with earthquakes as the dominant environmental loads for structures [14,20]. The past decade has seen increased Atlantic hurricane activity with enormous economic losses [11,17]. During hurricanes, damage to building's roofs is mostly due to uplift forces. The ability to withstand uplift forces caused by wind across the roof surface is one of the critical design aspects.

Flat roofs are commonly used in many commercial structures, offices, apartment complexes, podiums as part of high rise buildings and residential buildings. Wind across the roof produces uplift forces at the roof surface which may cause catastrophic roof failure under extreme wind conditions [19,5,6,10]. It is common to see use of loose concrete roof pavers with these flat roofs. The pavers are also being used more and more as additional landscaping elements, path ways on vegetated roofs (green roofs) and as mitigation element for preventing uplift of vegetative materials due to their relatively heavy dead-weight. The loose-laid roofing pavers utilize gravity ballasting in lieu of anchors or adhesives [9,4]. In certain zones of the roof, (i.e., windward edges, corners, and eaves), wind flow may cause large drop in air pressure above the paver's surface. The resultant pressure difference on individual tiles (net pressure, which is the difference between external and underneath pressures) creates an uplift force. In case of loose paver roofs, the uplifting force can only be countered by the weight of the individual paver itself. This means, for scenarios in which the uplift force is higher than the individual weight of the paver, dislodgement may occur, resulting in roof failure and airborne missiles.

The determination of the wind speed limits at which loose pavers initiate dislodgement has important economical and safety implications. Aside from its economy in areas where abundant, roof paver has demonstrated a propensity for failure, while under less severe conditions, it may become an airborne missile when under extreme wind conditions. Being airborne missiles, roof pavers may lead to successive failure to the surrounding building environment. For the above reasons, a number of studies have been developed for the estimation of the uplifting forces on the pavers [9,4] and hence finding suitable securing techniques are needed.

In addition to wind tunnel tests, full-scale testing and measurement of wind effects play an important role. Effective studies of wind effects on full- and large-scale building models have been limited. Nevertheless, full-scale measurements have provided valuable findings and data, and contributed to the validation or otherwise of certain wind tunnel techniques. Useful wind load data have been collected on roofs of residential homes during hurricanes through the Florida Coastal Monitoring Program (FCMP) (see http://users.ce.ufl.edu/~fcmp/overview/house.htm). Researchers at International Hurricane Research Center (IHRC) of Florida International University (FIU) developed a new full-scale testing facility, the Wall of Wind (WoW) (see Fig. 1a), to enhance our capabilities to test under hurricane wind forces [12,13,2,3] and rain [7].

Full-scale testing is advantageous in the general context of wind engineering tools for the following reasons: (1) adverse scaling effects (such as those due to violation of Reynolds number similitude) can be reduced, (2) some building components (such as roof tiles and pavers) are too small in size to be reproduced in wind tunnel model scale tests but can be prototyped without any distortion in full-scale tests, (3) full-scale tests under wind flows with speeds comparable to those of destructive hurricanes can examine the structural integrity of building components and their connection/mounting mechanism. Some disadvantages of full-scale testing are: (1) the test model and overall testing costs are high, (2) only low-rise structures can be tested due to the wind field size limitation of the facility and blockage effects, (3) only isolated testing can be performed without modeling the surroundings as usually done in wind tunnels.

* Corresponding author at: Department of Civil and Environmental Engineering, University of Western Ontario, London, ON, Canada. Tel.: +1 519 661 2111x88028; fax: +1 519 661 3339.
E-mail address: gbitsuam@UWO.ca (G.T. Bitsuamlak).
0141-0296/$ - see front matter
http://dx.doi.org/10.1016/j.engstruct.2012.05.008

The purpose of this study is to assess the aerodynamic windloads acting on a concrete roof paver using the full-scale 6-fan WoW at IHRC of FIU. Experimental tests were conducted on fullscale pavers mounted on a test building model in order to evaluate the wind-induced external and underneath pressures acting on the pavers. The aim of the study is to help better understand external and underneath pressure distribution over blasted roof system (in this case concrete paver roofs) through experimental testing for more effective protection against damage caused by the wind. The study provides the best possible locking arrangements of pavers, which would perform at high wind speeds, and bring improved paver qualities to the roofing industry.

2. Methodology

The full-scale six-fan WoW facility at FIU (see Fig. 1a) was used to generate the wind field for the present study. The 6-fan WoW can generate a category I Saffir–Simpson Scale hurricane wind speed that reasonably replicates mean wind speed and turbulence characteristics of those of real hurricane winds [15,7,12,13]. A combination of passive flow management devices and active controls allowed the 6-fan WoW to generate a suburban terrain mean wind profile (target power law coefficient value was α = 1/4.0). The longitudinal and vertical turbulence intensities measured at typical low-rise model roof eave height were 24% and 7%, respectively. The mean wind and turbulence intensity profiles are shown in Fig. 2a–e. The integral length scale (L_u^x) at typical low-rise building roof eave height was 90 m. This value was comparable to the estimated mean value of 98 m based on tropical cyclone wind data collected through Florida Coastal Monitoring Program (FCMP) [21]. The longitudinal and vertical power spectral densities at y = 3.66 m and z = 3.35 m, and a comparison with the FCMP, the revised Kaimal and the Panofsky models (see [15,20] are shown in Fig. 3; it worth noting that the quasi-periodic waveform (W2) was used in the present study. The satisfactory reproduction of turbulence parameters is essential for simulating realistic aerodynamic responses (such as peak pressures). For more detailed information on the 6- fan WoW configuration, its flow characteristics (including the wind turbulence spectra), and comparisons with tropical cyclone flow characteristics, see Huang et al. [15].

A test building was constructed to support the full-scale concrete pavers (a total of 25) in a similar way to real roof concrete pavement system (see Fig. 4a). The size of the test building model was 10 ft width 10 ft depth 7 ft height (3.05 m width 3.05 m depth 2.13 m height) which was engulfed completely in the 22 ft wide 16 ft high (6.71 m wide 4.9 m high) wind field generated by the WoW as described in Fig. 2a. The concrete paver has a dimension of 2 ft by 2 ft with 2 in. thickness (61 cm by 61 cm with 5.1 cm thickness). The spacing between the underneath of the paver and the roof deck is 1 ft. The whole test model represents a generic roofing system for a flat roof of a low-rise building without a parapet wall. Pressure taps were installed on the roof paver and underneath it (Fig. 4a) to measure both external and underneath pressure simultaneously. Fig. 4b shows the external and underneath pressure tap layout. The pavers are named alphabetically from A to Y. As shown in Fig. 4b, all the 25 roof pavers were instrumented for both external and underneath pressure measurements. Underneath pressure taps are referred to on the figure by hollow circles and external pressure taps with solid circles. The underneath and external pressures were measured using SETRA low pressure transducers (see Fig. 5). A total of 63 transducers were used. Each transducer has two ports, a reference pressure port and a port connected to the pressure tap at location of interest to measure the fluctuating pressures (external or underneath). The differential pressure which resulted in the data acquisition (DAQ) system in a voltage ranging from 0 to 5 V was calibrated and converted into PSI. The transducers have a measuring range of ±1.8 PSI and allow for data collection at sampling rate of 100 Hz. To ascertain the highest level of accuracy in the measurements, on-site calibration was conducted for each transducer.

Wind speeds were measured at the eave height of the test model (i.e. at 7 ft height (2.13 m)) using a turbulent flow Cobra probe. A fixed frame was used to which the probe could be secured. The frame was built using a system of steel tubes connected together (see Fig. 1b) and fixed to the ground. In order to get the reference wind speed, velocity measurements were taken without the presence of the test structure as the structure would have affected the wind. A quasi-periodically varying wind speed was used for the tests [15]. The wind had duration of about 3-min average with a 3 s mean wind speed of about 63.7 mph

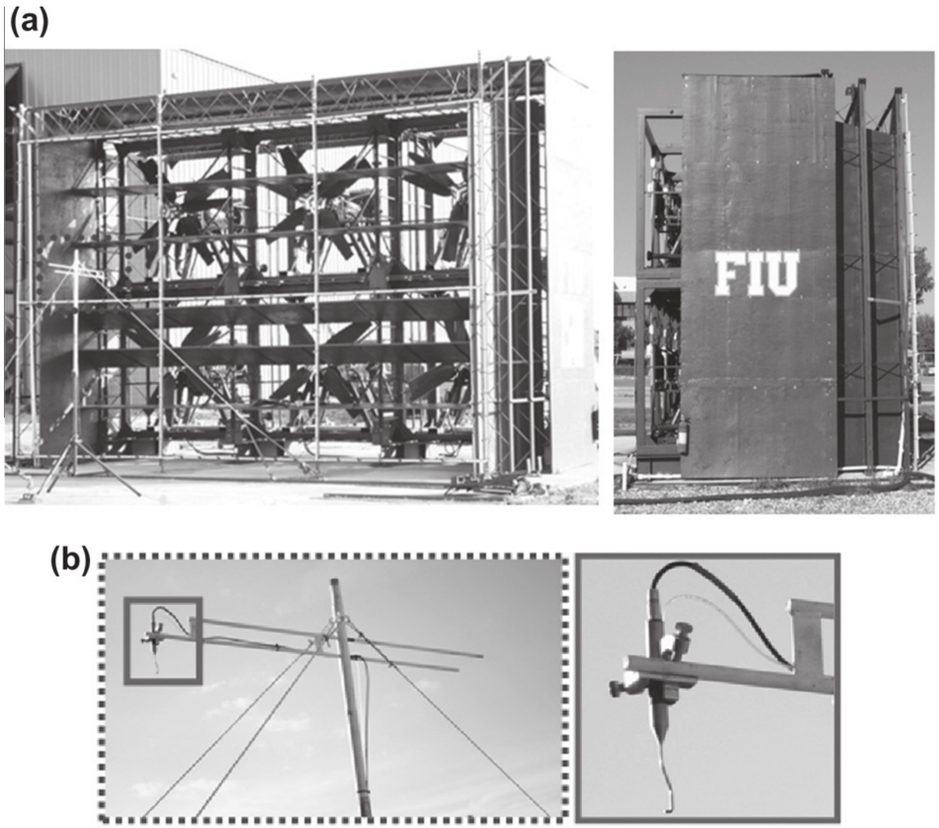

Fig. 1 Wall of Wind (WoW): (a) six-fan WoW, (b) turbulent flow Cobra probe mounted to assess the full-scale wind

(28.48 m/s) and the turbulence intensity was about 27%. The mean velocity and turbulence profiles were earlier described in Fig. 2a–e.

The test model was secured in front of the WoW (see Fig. 6) and tested for five wind directions (0 deg, 22.5 deg, 45 deg, 67.5 deg, and 90 deg). This allowed finding the most critical wind exposure that may cause excessive wind loads on individual roofing pavers. Pressure data were acquired at sampling frequency of 100 Hz for a period of three minutes. Pressure data were collected for each individual test as one minute before and a minute after the 3-min tests (baseline measurements). The average of the two mean values of the one minute measurements before and after each test (baseline) was measured and monitored to avoid natural wind effects to influence the results being sought.

Time history and spectrum of pressure data collected from one pressure tap are shown in Fig. 7a. The effects of the cutoff frequency on the measured pressure were investigated for a tap location exhibiting high pressure magnitude. Representative results are shown in Fig. 7b and Table 1. It can be seen that both the peak (minimum value) and (fluctuation) rms of the roof pressure can be significantly affected by the low-pass filtering when the cutoff frequency is lower than 30 Hz. Although further systematic investigations are needed to generalize this result, it is tentatively concluded that the pressure fluctuations are not significant if frequency contents higher than 30 Hz are considered.

3. Results and discussion

At the location of each pressure tap, the time history of the pressure coefficient, $Cp(t)$, is obtained from the time history of the measured differential pressure, $p(t)$, as

$$Cp(t) = \frac{p(t)}{\frac{1}{2}\rho U_3^2}$$

where ρ is the air density at the time of the test (1.16 kg/m^3) and U_3 is the highest observed peak 3-s wind speed measured at the eave height of the test model over a time period of three minutes. The 3-s wind speed was 28.48 m/s (63.7 mph). The pressure data are recorded during the test in PSI (Pressure in Pa = 6894.76 [Pressure in PSI]). Referring to the data vector of the pressure coefficients over the sampling time period as Cp, the mean value of the pressure coefficients at any location, Cp_{mean}, is defined as

$$Cp_{\text{mean}} = \frac{1}{n}\sum_{i=1}^{n} Cp_i$$

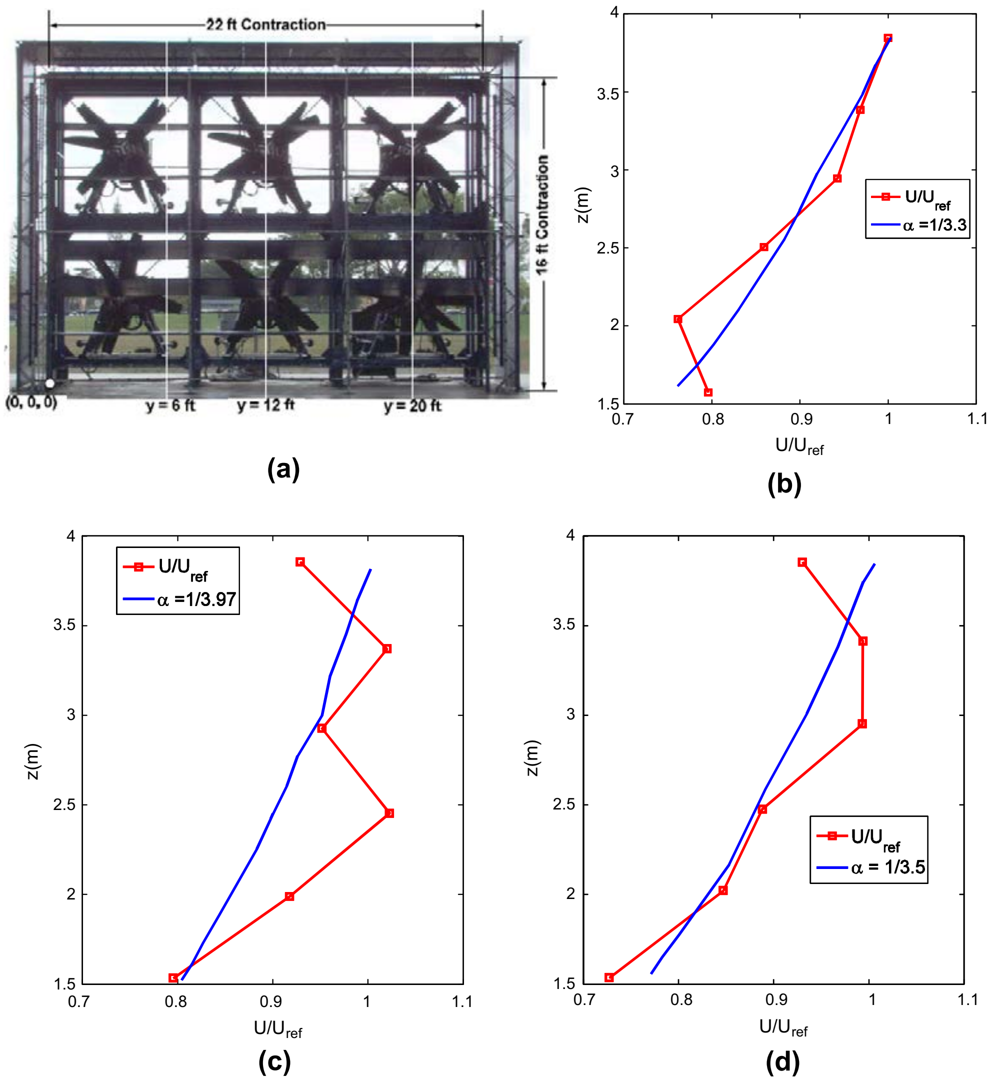

Fig. 2. Full-scale 6-fan WoW (a), a non-dimensional mean velocity profiles at y = 1.22m – 4ft (b), at y = 3.66m – 12ft (c), at y = 4.27m – 14ft (d), and longitudinal (e) and vertical turbulence profile (f) at y = 3.66m (12ft).

where n is the number of measurements in the sample. The root mean square value of the pressure coefficients is defined as

$$Cp_{\mathrm{rms}} = \left[\frac{1}{n}\sum_{i=1}^{n}(Cp_i - Cp_{\mathrm{mean}})^2\right]^{\frac{1}{2}}$$

The minimum pressure coefficient values (Cp_{min}) are obtained from the measured pressure time histories. However, these observed peaks can exhibit wide variability from one realization to another due to the highly fluctuating nature of wind pressures. This means that significant differences might be expected in the peak values of pressure time series obtained from several different tests under nominally identical conditions. Therefore it is generally preferable to use a more stable estimator for the expected peaks. To remove the uncertainties inherent in the randomness of the peaks, probabilistic analyses were performed using an automated procedure developed by Sadek and Simiu [18] for obtaining statistics of pressure peaks from observed pressure time histories. Because estimates obtained from this approach are based on the entire information contained in the time series, they are more stable than estimates based on observed peaks (see also [3].

Surface plots of the mean, root mean square, and observed negative peak (min) values of the external pressure coefficients (Cp_{mean}, Cp_{rms}, and Cp_{min}) acting on the external surface of the paver roof are shown on Fig. 8a–c for 0 deg. Fig. 9 shows the estimated minimum values for the external pressure coefficients acting on the roof for different wind exposures. For the evaluation of the estimated minimum values of the pressure coefficients, a time period of 1 h and 95% confidence were considered. For all of the possible wind directions, results show that pavers close to the edges and corners of the roof are subjected to comparatively high negative pressures. This is mainly due to the wind-induced conical vortices (e.g., [5,10].

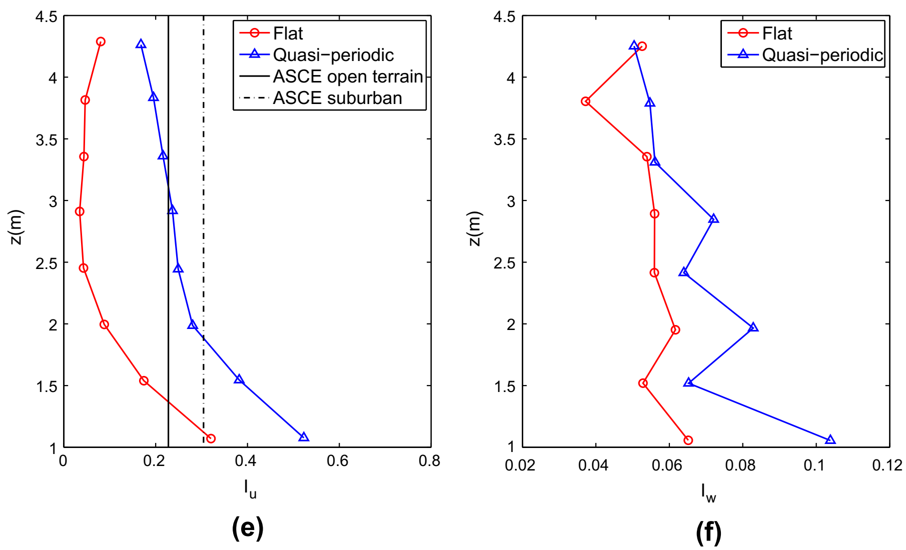

Fig. 2 (*continued*)

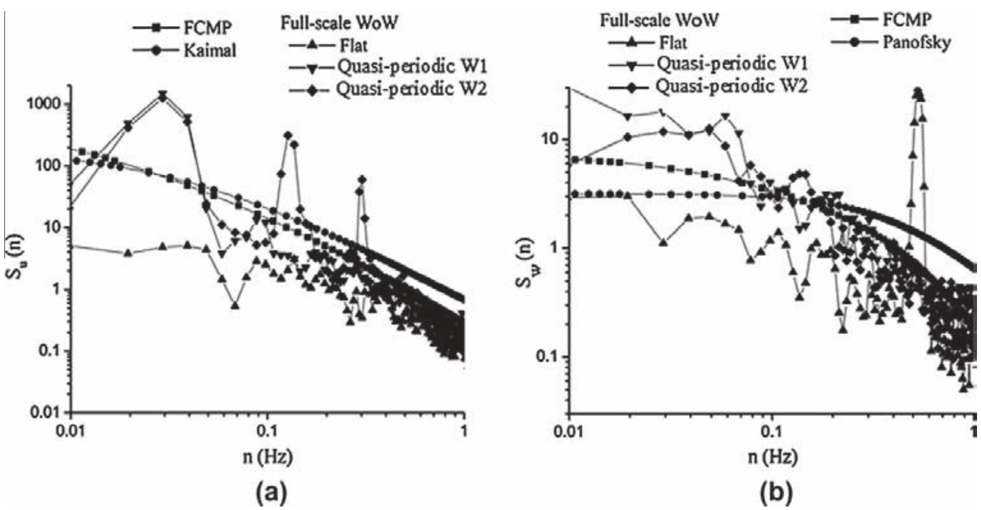

Fig. 3. Power spectral densities for revised full-scale WoW (z = 3.35m, y = 3.66m): (a) longitudinal power spectral density plots, (b) vertical power spectral density plots. Note that quasi-periodic W2 was used in teh present study.

The values of the pressure coefficient are highly dependent on wind direction. Among all of the possible wind exposures, results show that directions 22.5 deg and 67.5 deg are the most critical. Measured values of Cp_{min} and Cp_{rms} should be considered for the proper securing of individual pavers, as wind-induced damage on building pavers may occur either due to local peak wind loads, that is, by exceeding the ultimate capacity, or due to fatigue caused by repetitive loads.

Compared to external pressures, the values of underneath pressures acting on the lower surfaces of the pavers are low. The pressure distribution produced by the wind flow over the outer surface of the roof produced secondary flows through the spaces between the paver elements and underneath the elements. A pressure distribution is thus established under the roof pavers. This pressure distribution is related to, but different from, that on the outer surface. In fact, underneath pressure exhibits more uniformity compared to external pressure distribution. Fig. 8d–f shows mean (Cp_{mean}), root mean square (Cp_{rms}), observed minimum (Cp_{min}) values of the underneath pressure coefficients distributed over the inner surface of the paver roof.

In designing the roof it is necessary to determine, the pressure differential on the individual pavers. The total pressure coefficient at any location, $Cp_{tot}(t)$, is the instantaneous difference between the external pressure coefficient, $Cp_{ext}(t)$, and the corresponding underneath pressure coefficient, $Cp_{int}(t)$, at the same locations

the net design total pressure can be obtained as

$$Cp_{\text{tot}}(t) = [Cp_{\text{ext}}(t) - Cp_{\text{int}}(t)],$$

$$P_{\text{tot}}(t) = \frac{1}{2}\rho U_3^2 [Cp_{\text{ext}}(t) - Cp_{\text{int}}(t)]$$

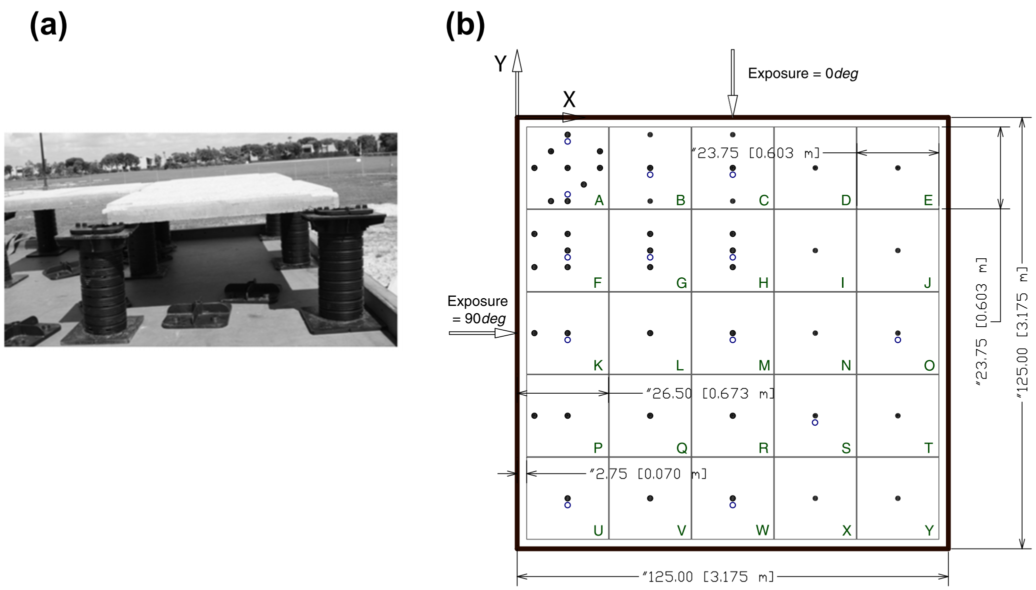

Fig. 4. Paver roof test model: (a) under construction, (b) pressure tap and paver layout (solid circles designate external taps, hollow circles designate underneath taps).

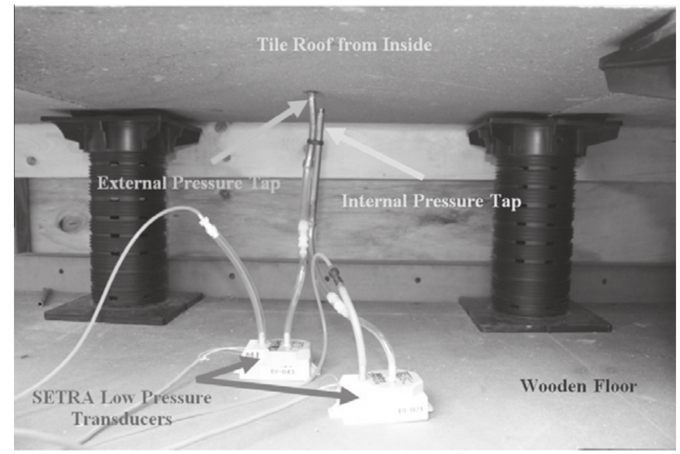

Fig. 5. SETRA low pressure transducers used for external and underneath pressure measurements.

Cutoff freq.	Mean (Pa)	Min (Pa)	rms (Pa)
Unfiltered (50)	−208.223	−1419.64	166.8542
30	−208.223	−1339.66	162.0278
20	−208.223	−1262.44	157.2014
10	−208.223	−1125.92	150.3066
5	−208.223	−834.96	143.4118
1	−208.223	−702.58	132.3802
0.5	−208.223	−612.948	128.9328
0.1	−208.223	−492.289	111.0063
0.05	−208.223	−400.588	105.4904

Table 1. Effect of filtration on the statistical parameters of the raw pressure data measured at tap 4 on paver A of Fig. 4.

where ρ is the air density which may be assumed to be 1.25 kg/m^3, U_3 is the peak 3-s wind speed in m/s. The design wind speed for houses in the Miami region is usually taken as U_3 = 146 mph (65.27 m/s). In certain areas of the roof, pressure differences (i.e., differences between external and underneath pressures) produce uplift on the elements that, at design wind speeds, can be greater than the weight of the individual paver. Two explanatory examples are provided below.

3.1. Design wind loads for a single paver

The external pressure coefficient distribution over the roof paver system indicates that paver **A** is subjected to the worst load for 67.5 deg angle of attack. To properly secure such pavers in place, it is necessary to know the wind-induced loads acting on each individual paver under the design wind speed.

Fig. 10 shows the external and the net pressure distribution over the surface of paver A. The figure shows the spatial distribution of the instantaneous

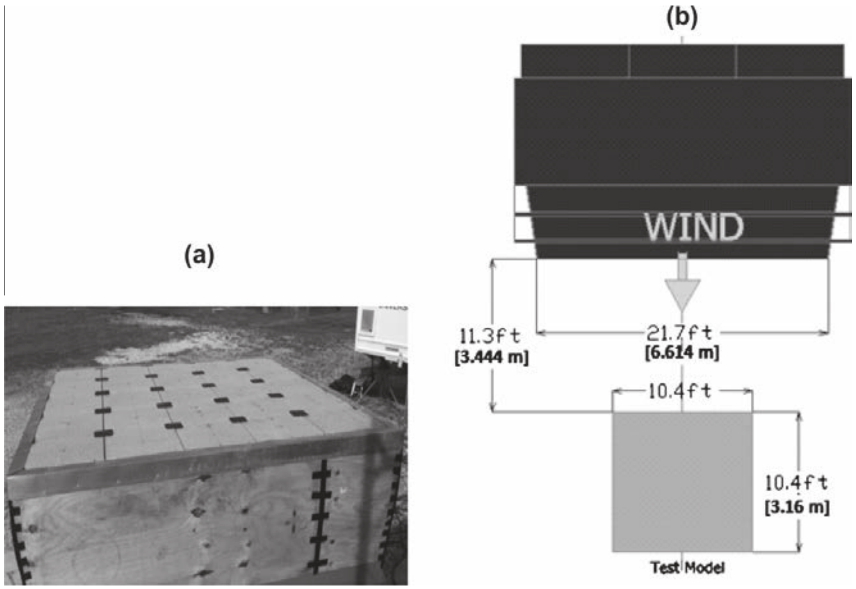

Fig. 6. Paver roof test: (a) complete model, (b) layout of the test model and the WoW (height of the wind field is 16ft; height of the test model is 7ft; 1ft = 0.3048m).

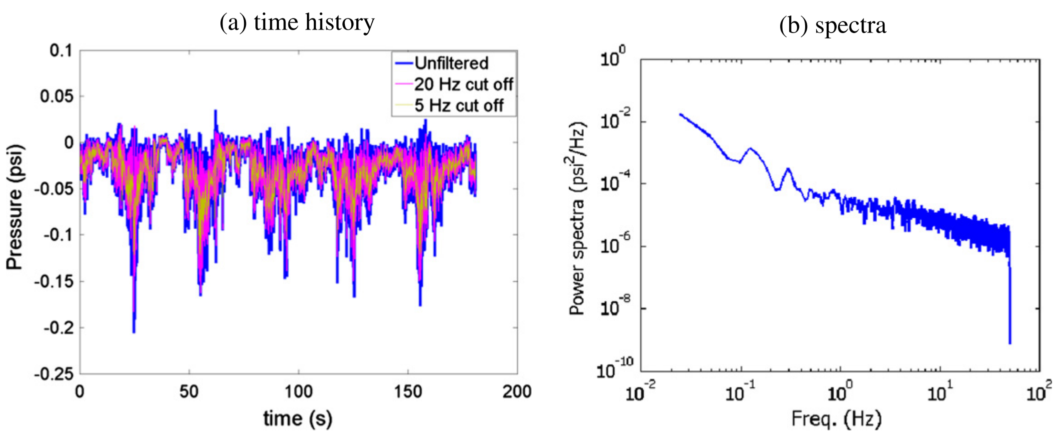

Fig. 7. Effect of filtration on the pressure measured at tap 4 on paver A of Fig. 3b.

pressure coefficients over the paver surface at the instant when observed area-average pressure coefficient reached minimum value. It is to be noted that the imperfect spatial coherence of the velocity fluctuations (such as in the present case) may result in reductions of the overall wind effects (such as area-averaged pressures) with respect to the case of perfectly coherent flows. For large building components those reductions are significant. However, for components with sufficiently small dimensions (such as the roof pavers in this study) the reductions are hypothesized to be relatively small. Detailed analyses on correlation will be performed in future to test this hypothesis for roof pavers and extend the findings to the net pressures at the edges.

Fig. 10 shows that the underneath pressure contributes to a reduced net pressure compared to the external pressure. For example for paver A the mean pressure may have been overestimated by about 15% if the underneath pressure was not measured. The surface of the paver close to the left edge is subjected to higher suction than the surface close to the right edge. This means that the overall uplifting force is not acting at the center of the paver but close to the left edge. Therefore even for cases where the total uplift force is less than the weight of the paver, the corresponding overturning moment may not be resisted by the weight of the paver. This situation may be critical under relatively high wind speeds, and be followed by drag forces causing the paver to become wind-borne.

The time history of the overall wind load, F_A, acting on any single paver was obtained from the time history of the total pressure coefficients as follows:

$$F_A(t) = \frac{1}{2}\rho U_3^2 \left[\frac{1}{n_a}\sum_{i=1}^{n_a} Cp_{\mathrm{tot},i}(t) \times A_i\right]$$

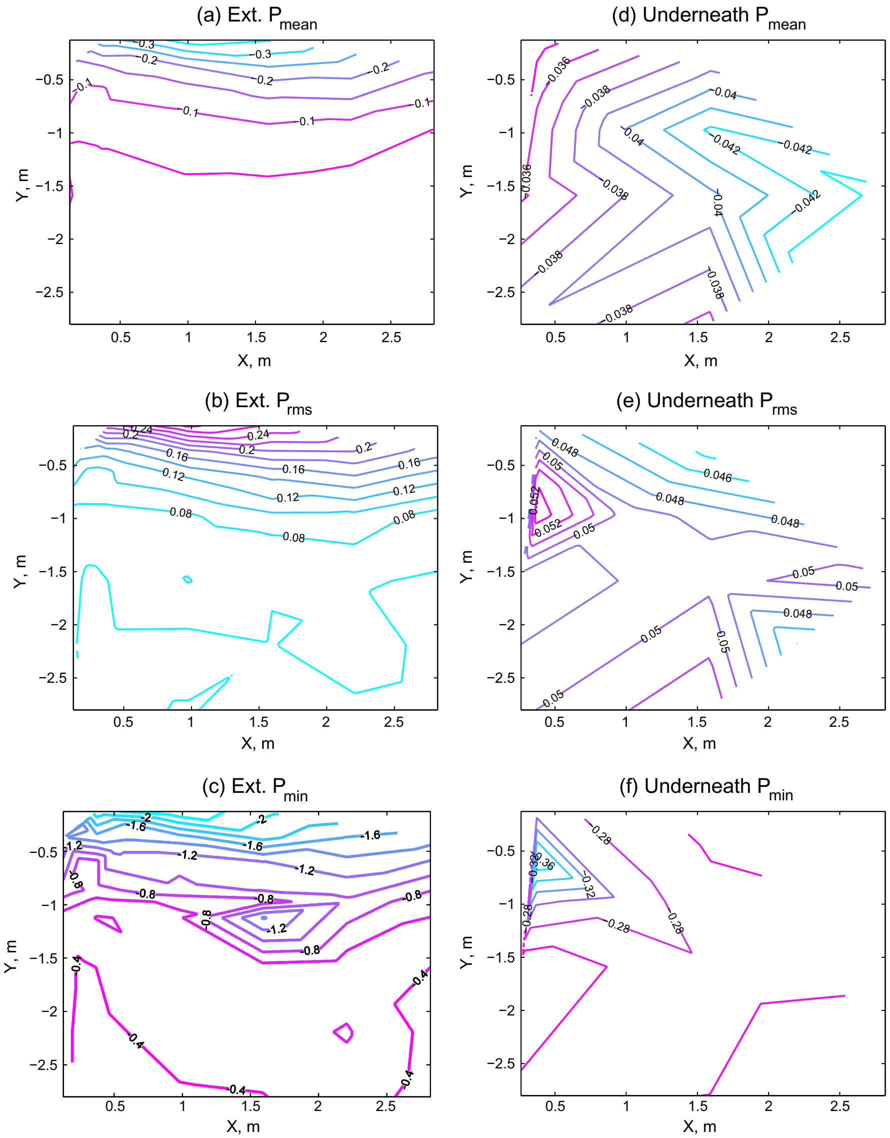

Fig. 8. External (a-c) and underneath (d-f) pressure for 0 deg angle of attack over the whole roof.

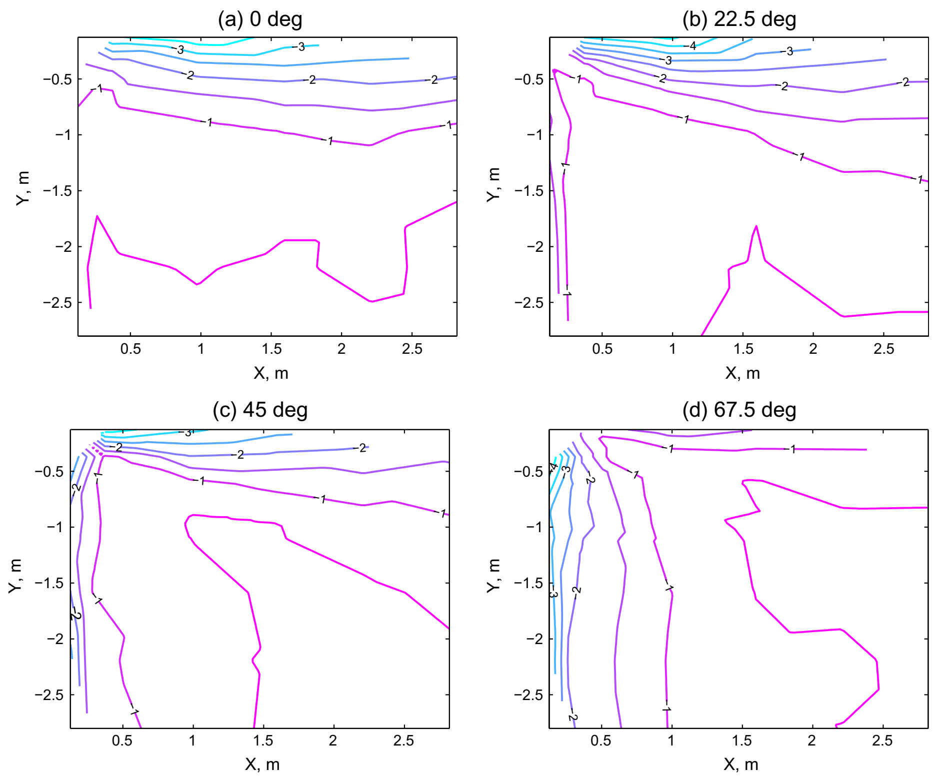

Fig. 9. Estimated Cp_{min} (external pressure) for four different angles of attacks over the whole roof.

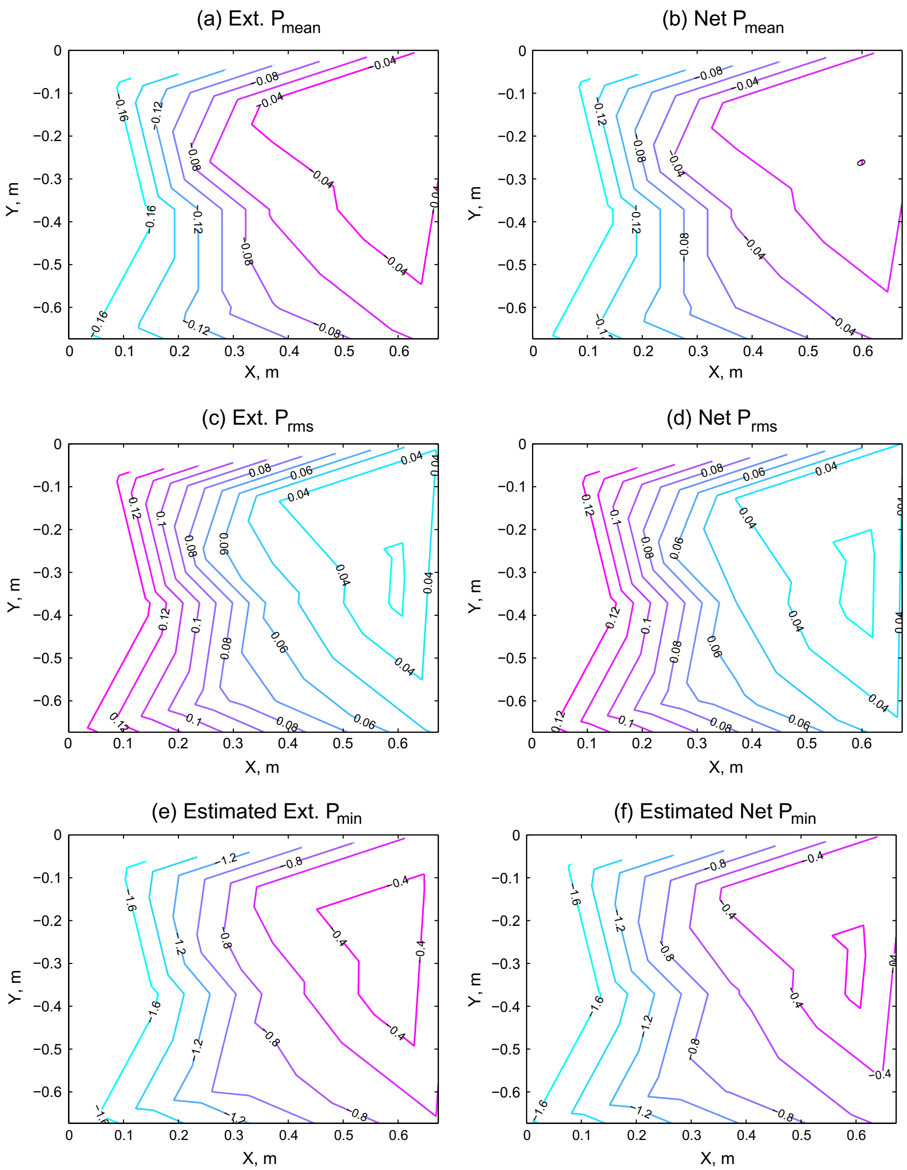

Fig. 10. Distribution of the external and net pressures (PSI) on paver A for 67.5 deg angle of attack.

where n_a is the total number of external pressure taps on the paver, A_i is the tributary area of the tap i, and $Cp_{tot,i}(t) = [Cp_{ext,i}(t) - Cp_{int,i}(t)]$ is the net total pressure coefficient at the external pressure tap number i for the single paver at any time t.

Similarly, the overturning moment caused by the wind about the right edge, $M_A(t)$ (see Fig. 11a), was obtained from

$$M_{A,o-o}(t) = \frac{1}{2}\rho U_3^2 \left[\frac{1}{n_a}\sum_{i=1}^{n_a} Cp_{\mathrm{tot},i}(t) \times A_i \times d_i\right]$$

where d_i is the moment arm which can be defined as the distance between the centroid of the tributary area A_i and the edge o–o. Tributary areas for each external pressure tap on the surface of paver **A** are schematically presented in Fig. 11b. The values of the tributary areas in m² and in.² along with the corresponding moment arms about the edge o–o are given in Table 2.

Fig. 11 provides the total wind uplift force and overturning moment acting on paver **A** for 67.5 deg angle of attach as a function of wind speed (peak 3-s gust) in terms of mean, rms, observed peak, and estimated peak. It was observed that the values of the uplifting force and overturning moment increase with the increase in the wind speed. The uplifting force and overturning moment at the de sign Fig. 12 wind speed [U3 = 146 mph (65.27 m/s)] for Miami down town region for example was observed to be greater than the counterbalancing weight and the corresponding resisting moment of the paver.

3.2. Design wind loads for a group of pavers locked together

In order to evaluate the efficacy of locking a group of pavers together, the net wind-induced uplift force acting on a group of four pavers was determined as a function of the 3-s gust wind speed.

Fig. 13a shows the net mean, rms, observed peak, and estimated peak uplifting wind-induced force acting on a group of four pavers (**A, B, F,** and **G** as indicated in Fig. 4b). The figure shows that at the design wind speed [146 mph (65.27 m/s)], both of observed and estimated peak forces are higher than the overall resisting force due to weight (~1.886 kN). This means that connecting pavers together into groups of four elements is not sufficient to withstand the wind-induced uplifting force at design wind speed.

Fig. 13b shows the net mean, rms, observed peak, and estimated peak uplifting wind-induced force acting on a group of nine pavers (**A, B, C, F, G, H, K, L,** and **M** as indicated in Fig. 4b). The figure shows that, at design wind speed [146 mph (65.27 m/s)], both of observed and estimated peak forces are lower than the overall resisting force due to weight [~954 lb (4.244 kN)]. This means that connecting pavers together into groups of nine elements was found to be sufficient to withstand wind-induced uplifting force at design wind speed.

In conclusion, a technique for locking a group of pavers together can be used to create a paver group acting together to create sufficient counterbalancing weight even for net uplifting force expected at high velocity wind zones such as Miami. However, in order to have additional safety, for high velocity zones it is recommended that the locking system should be able to hold a group of at least 4 x 4 or 5 x 5 pavers together. The performance of the locking system to maintain a group of pavers connected together under any arbitrary force or moment (that is enough to cause uplifting of the group as one rigid body) applied at, but not limited to, the center of the group should be tested by the designer (i.e., the group of pavers should be held together as if it was one rigid body). This condition should be guaranteed over the expected life of the roof.This means that the locking system itself may require additional maintenance or replacement due to member aging or windinduced fatigue loading. It is also important to maintain the gap between the pavers (about 0.2 in. (0.005 m) between each two neighbor pavers) to take the advantage of the reduction of the net uplift due to the underneath pressure. Since dirt or movement of the pavers with aging can close the gaps it will be safer to design based on external pressure alone unless there strict maintenance/cleaning program in place. Neglecting or eliminating this gap may result into group net uplifting force that is higher than the one predicted by the current study.

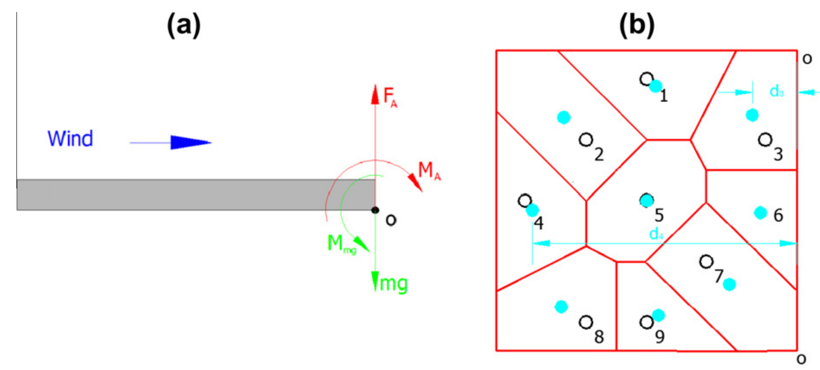

Fig. 11. Analysis of paver A under wind loads: (a) free body diagram, (b) tributary areas for external pressure taps (hollow circles designate tap positions; solid circles designate the centroid of each area).

4. Comparison with ASCE 7-2005

Following the procedure of Section 6.4 of ASCE 7-2005 [1] for rigid buildings, the wind uplift force on tile A is calculated for the following conditions:

i Basic wind speed 146 mph (65.27 m/s).
ii Building classification: category II importance factor (I = 1) (see page 77 of the standard).
iii Exposure: category B (suburban terrain).
iv Height exposure adjustment coefficient 1: from page 40 of the standard, λ = 1.
v Simplified design wind pressures, p_s, for the Main Wind-Force Resisting System (MWFRS) of low-rise simple diaphragm buildings represent the net pressures (sum of internal and external) to be applied to the horizontal and vertical projections of building surfaces.
vi $p_s = \lambda I p_{s30} = 1.0 \times 1.0 \times p_{s30}$ (Eq. (6-1) of the standard, p. 24).
vii Roof tile A design pressure: from page 43 of the standard, tile A lies totally in zone 3, effective wind area of the paver is 4 ft^2 (0.37 m^2), for V = 146 mph.

$$p_s = \lambda I p_{s30} = 1.0 \times 1.0 \times (-95.5) = -95.5 psf$$

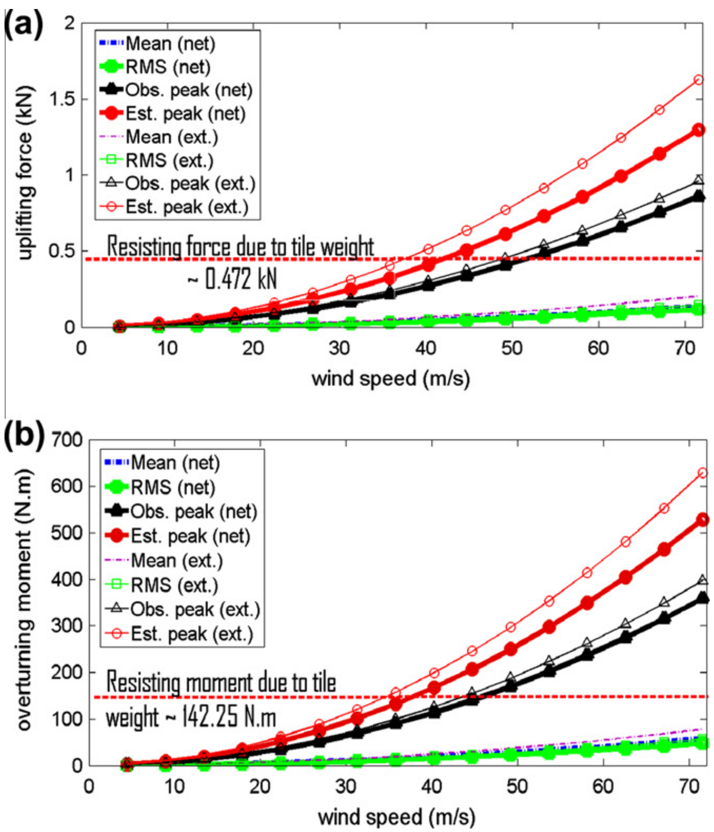

Fig. 12. Wind loads acting on paver A for 67.5 deg angle of attack versus 3 s gust wind speed: (a) uplifting force, (b) overturning moment.

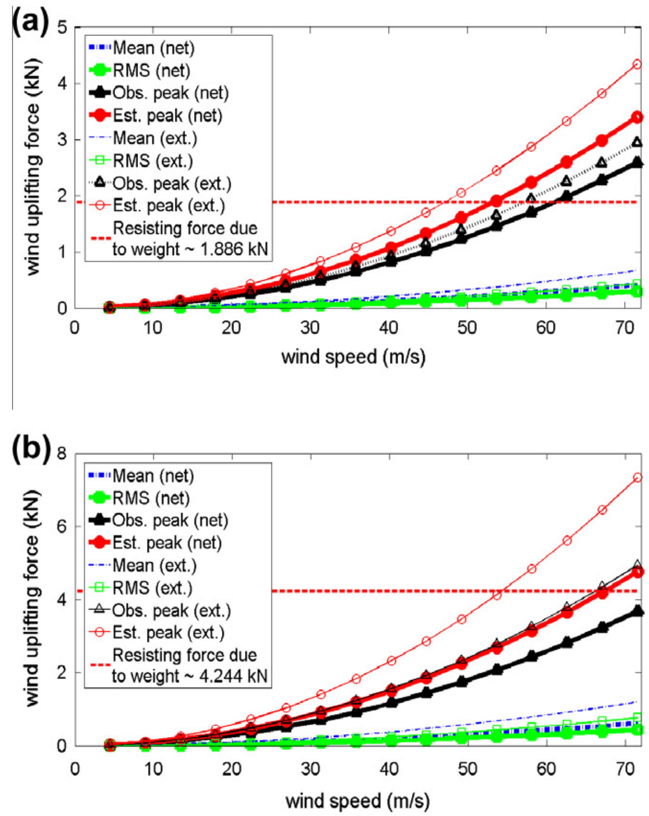

Fig. 13. Wind loads acting on pavers for 67.5 deg angle of attack: (a) A,B, F, G as a group, (b) A, B, C, F, G, H, K, L, and M as a group.

which gives the total uplift force on tile A as:
95.5 x 2 x 2 = 382 lb = 173.3 kg = 1.7 kN.

The external wind load (i.e. external pressure only) on tile A from the present study is 1.5 kN (see Fig. 12a.) which is close to the value predicted by ASCE 7-2005 with 12% difference. However when the effect of internal pressure was considered, the net wind load from the present study is 1.35 kN (see Fig. 12a). This reveals that the internal pressure contributes towards reducing the total uplift wind load.

5. Conclusion

Full-scale aerodynamic tests were carried on concrete roof pavers at the Wall of Wind to evaluate the external and underneath pressure coefficient distribution on the pavers. The pressure coefficients at various locations on the roof paver system were evaluated for five different wind directions. Among the tested cases,the 22.5 deg and 67.5 deg angle of attack produced the highest pressure coefficients. At the corners and edges of the paver roof system, the net pressure difference produced uplift forces, at the design wind speed, that were greater than the weight of the individual paver.

Taps number	Tributary area		Moment arm	
	m^2	$in.^2$	m	in.
1	0.0401	62.12	0.2840	11.18
2	0.0513	79.56	0.4684	18.44
3	0.0422	65.46	0.0899	3.54
4	0.0406	62.90	0.5314	20.92
5	0.0423	65.64	0.3030	11.93
6	0.0280	43.34	0.0737	2.90
7	0.0511	79.16	0.1361	5.36
8	0.0415	64.35	0.4735	18.64
9	0.0270	41.85	0.2781	10.95

Table 2. Tributary area and distance from tap centroid to line o-o for each individual tap on paver A.

Considering the fact that the wind may blow from any direction, all the pavers close to the edges and corners of the roof should be properly secured. The present study shows that by locking a group of loose pavers together produced sufficient weight that acts together to counterbalance the net uplifting loadings caused by the wind. It is recommended to use a locking system that will be able to hold a group of at least 4 x 4 or 5 x 5 pavers together.

In addition, comparisons between the results obtained in this study for external pressure only and the values predicted by the ASCE 7-2005 shows close agreement. The contribution of underneath pressures to the net pressure was observed to be significant (15% reductions were observed in the present study). This indicates that future measurements of underneath pressures are indispensable. The results of the research reported in this paper will enable the design and development products and appropriate criteria for the securing of the roof pavers safely.

Acknowledgments

The help offered by the Wall of Wind manager, Walter Conklin and the Research scientist, Roy Liu Marquis is greatly acknowledged. We would also like to acknowledge the great help received from our graduate research assistants (Amanuel Tecle, Francis Bain, Ruilong Li, Carlos Guerra, Serge Fueze and Zak Lata).

References

[1] ASCE 7-2005. Minimum design loads for buildings and other structures. ASCE Standard, ASCE/SEI 7-05, American Society of Civil Engineers, Virginia; 2006.

[2] Aly AM, Gan Chowdhury A, Bitsuamlak G. Wind profile management and blockage assessment for a new 12-fan WoW facility at FIU. Wind Struct, Int J 2011;14(4):285–300.

[3] Aly AM, Bitsuamlak G, Gan Chowdhury A. Florida International University's Wall of Wind: a tool for the improvement of code provisions and design criteria for hurricane-prone regions. In: Vulnerability, uncertainty, and risk: analysis, modeling, and management – proceedings of the ICVRAM 2011 and ISUMA 2011 conference; 2011. p. 352–9.

[4] Bofah KK, Gerhardt HJ, Kramer C. Calculations of pressure equilibration underneath loose-laid, flow permeable roof insulation boards. J Wind Eng Ind Aerodyn 1996;59:23–37.

[5] Bienkiewicz B, Sun Y. Local wind loading on the roof of a low-rise building. J Wind Eng Ind Aerodyn 1992;45:11–24.

[6] Bienkiewicz B, Sun Y. Wind loading and resistance of loose-laid roof paver systems. J Wind Eng Ind Aerodyn 1997;72:401–10.

[7] Bitsuamlak GT, Gan Chowdhury A, Sambare D. Application of a full-scale testing facility for assessing wind-driven-rain intrusion. Build Environ 2009;44(12):2430–41.

[8] Blessing C, Gan Chowdhury A, Lin J, Huang P. Full-scale validation of vortex suppression techniques for mitigation of roof uplift. Eng Struct 2009;31(12):2936–46.

[9] Gerhardt H, Kramer C, Bofah KK. Wind loading on loosely laid pavers and insulation boards for flat roofs. J Wind Eng Ind Aerodyn 1990;36:309–18.

[10] Kawai H, Nishimura G. Characteristics of fluctuating suction and conical vortices on a flat roof in oblique flow. J Wind Eng Ind Aerodyn 1996;60:211–25.

[11] Emanuel K. Increasing destructiveness of tropical cyclones over the past 30 years. Nature 2005;436(7051):686–8.

[12] Gan Chowdhury A, Aly AM, Bitsuamlak GT. Full- and large-scale testing to promote wind disaster mitigation. In: The Fifth US–Japan (UJNR) Workshop on Wind Engineering, Chicago, USA; July 26–28, 2010.

[13] Gan Chowdhury A, Bitsuamlak GT, Simiu E. Aerodynamic, hydro-aerodynamic, and destructive testing. J Inst Civil Eng 2010;163(2):137–47.

[14] Holmes DJ. Wind loading of structures. London: Spon Press; 2001.

[15] Huang P, Gan Chowdhury A, Bitsuamlak G, Liu R. Development of devices and methods for simulation of hurricane winds in a full-scale testing facility. Wind Struct 2009;12(2):151–77.

[16] National Science Board. Hurricane warning: the critical need for a national hurricane research initiative. NSB-06-115; 2007. p. 1–36.

[17] Pielke Jr RA et al. Normalized hurricane damage in the United States: 1900–2005. Nat Hazards Rev J ASCE 2008;9(1):29–42.

[18] Sadek F, Simiu E. Peak non-Gaussian wind effects for database-assisted lowrise building design. J Eng Mech 2002;128(5):530–9.

[19] Stathopoulos T, Baskaran A, Goh PA. Full-scale measurements of wind pressures on flat roof corners. J Wind Eng Ind Aerodyn 1990;36:1063–72.

[20] Simiu E, Scanlan RH. Wind effects on structures, fundamentals, and applications to design. 3rd ed. New York: Wiley-Interscience; 1996.

[21] Yu B, Gan Chowdhury A, Masters FJ. Hurricane power spectra, co-spectra, and integral length scales. Bound-Lay Meteorol 2008;129:411–30.

Series	Color	Reflectance	Emissivity	SRI
Shotblast	White 15	69.3%	.90	85
Shotblast	Beige 15	60%	.90	72
Shotblast	Tan 20	38.5%	.90	43
Shotblast	Coral 25	48%	.90	56
Shotblast	Gravel 30	24.3%	.96	27
Shotblast	Brown 40	27%	.90	27
Shotblast	Rust 50	25%	.90	25
Shotblast	Dark Grey 60	16%	.90	13
Granite	Light Grey 10	35.5%	.91	39
Granite	Salmon 20	29%	.90	30
Granite	Umber 30	21%	.90	20
Granite	Yellow 40	40%	.90	44
Granite	Red 50	25%	.90	25
Granite	Dark Grey 60	15%	.90	12
Fine	SP White 10	49.1%	.91	58
Fine	SP Cream 20	55%	.90	65
Fine	Sand 30	60%	.90	72
Fine	SP Stone 40	38%	.90	42
Fine	Light Grey 50	41%	.90	46
Fine	SP Grey 60	42%	.90	48
Fine	Ginger 70	45%	.90	52
Fine	Salmon 80	41%	.90	46
Fine	Tan 100	36%	.90	40
4C	Tawny 760	28.1%	.9	29
4C	Flint 765	18.1%	.9	14

HDG

BUILDING MATERIALS

Other opportunities to earn credits toward LEED Certification

- MATERIALS & RESOURCES CREDIT 4 - RECYCLED CONTENT
    - Recycled Glass
    - Recycled Porcelain
- MR CREDIT 5 (REGIONAL MATERIAL):
    - Within 500 miles of Rothschild, WI 54474

*Colors in blue can help toward SS Credit 7.1
*Colors in green can help toward SS Credit 7.2

Paver SRI

- Test Results

* SS CREDIT 7.1 (HEAT ISLAND EFFECT (NON-ROOF)): 29 or greater
* SS CREDIT 7.2 (HEAT ISLAND EFFECT (ROOF)): 78 or greater

CARE AND MAINTENANCE

MAINTAINING HDG TECH Sereis PAVERS

HDG TECH Series pavers can be maintained to retain the attractive appearance and prolong the life of the pavers. When using maintenance materials, please follow the product manufacturer's instructions regarding the use of any equipment or cleaning materials described here. Be sure to angle the spray and limit the pressure, as not to damage the surface of the paver when using a pressure washer. For specific or unusual problems, please call us at 503-360-9551.

WEEKLY MAINTENANCE

Sweep or pressure wash deck. In areas of high traffic, such as doorways, daily cleaning may be required.

SEMIANNUAL MAINTENANCE (SPRING AND FALL)

Power sweep, then pressure wash total deck surface. Spot clean any stained areas using procedures described in "Cleaning Heavily Soiled Areas."

Remove pavers located over drains on open joint systems. Clean debris from all drain covers to prevent plugging of drains and replace pavers.

Check pavers for rocking, low or high edges, joint spacing, alignment and broken or chipped pavers. If minor settling or movement has occurred, pavers can be leveled and adjusted with shims. Chipped or broken pavers should be replaced.

CLEANING HEAVILY SOILED AREAS

Soiled areas should be cleaned as soon as possible to avoid staining. The type of material causing the soiling determines the correct procedures.

A. Oil or Petroleum Products

Remove as much of the material as possible with hot water high pressure washer. Apply degreaser cleaner directly to the soiled area. With a stiff nylon brush or broom, scrub the area. Rinse the area with hot water high pressure washer. In some cases, a second cleaning may be required.

B. Rust Stains

Soak area with water. Scrub rust stains with masonry cleaner products per manufacturer's recommendations. (Be extremely careful around any metal surfaces.) Rinse area thoroughly.

C. Soiling from Normal Foot Traffic, Road Salts, Everyday Use

Wash area thoroughly with hot water high pressure washer. On heavily soiled areas, spray the area with a commercial grade cleaner and scrub with a nylon brush. Rinse thoroughly.

D. Gum or Tar

Apply dry ice directly on top of the gum or tar. After freezing, use a putty knife or scraper to remove the gum or tar from the surface.

E. Tobacco Stains on Light Colored Pavers

After pressure washing with hot water, saturate a paper towel with household bleach. Apply towel directly to stain and cover with minimum 3 mil poly. Tape poly to surface to hold in place. Leave stain covered for 24 to 48 hours. Remove to see if stain is gone or lightened. Repeat if necessary.

SNOW REMOVAL

Snow can be cleaned from the deck using shovels, walk-behind snow blowers or power brushes. A four wheeled garden tractor, weight not exceeding 1,700 lbs. manned, can also be used. Nylon or rubber scrapers are recommended to avoid scratching of pavers. Tire chains can cause minor scratching and extra care should be taken with chains.

The use of snow melt materials should be minimal and in accordance with manufacturer' s recommendations. Some types of snow melt are not recommended for use on new concrete and can cause surface damage to the paver.

OPEN JOINT INSTALLATIONS

Open joint installation is unique in that the pavers are elevated to allow water and air to flow through the joints of the pavers. It is essential that all the joints and all drains stay open, clean and free of dirt and debris. Failure to maintain clean joints may result in performance issues.

EFFLORESCENCE IN COLORED PAVERS

Efflorescence is a condition which appears as a white stain on some colored concrete and masonry products. It is a common occurrence in new concrete, created by sodium and sulfate compounds of several hydroxides, minerals, chlorides and nitrates which deposit on the surface and pores. It is the result of moisture evaporation and is most common on darker colored pavers and fabricated surfaces.

Water (rain, humidity, or ground water which "wicks") penetrates the pavers and dissolves latent salt. Sun draws the salt in solution to the surface and as moisture evaporates it is deposited on the surface. Efflorescence clears up as paver' s age and eventually dissipates. The length of time varies with weather conditions and wear. Efflorescence can also be caused when salts in the sub-base material wick up around and through the pavers and joints and deposit on the paver surface and sides.

HDG TILE WARRANTY

HDG Tile products are warranted to be free from defect in material and workmanship during manufacturing based on applicable industry standards. Warranty periods begin on delivery date of the warranted product and extend for the period listed below:

- Pavers are warranted for three years if properly installed according to both project specifications and HDG installation recommendations.

HDG

BUILDING MATERIALS

THE PRODUCTS OFFERED IN THIS CATALOG
ARE MANUFACTURED IN WAUSAU, WI, BY
HDG'S PARTNER FACTORY

HDGBUILDINGMATERIALS.COM

Concrete-based products with recycled glass or recycled porcelain may qualify for LEED credits that may contribute toward your project certification.